Journal of Energy Storage 82 (2024) 110514

Contents lists available at ScienceDirect

Journal of Energy Storage

journal homepage: www.elsevier.com/locate/est

Review article

State-of-the-art design of cathodes of multivalent batteries by electrospinning: A mini review on opportunities and challenges

Bahar Zare *, Sayed Khatiboleslam Sadrnezhaad *

Department of Materials Science and Engineering, Sharif University of Technology, Azadi Ave., P.O. Box: 11155-9466, Tehran, Iran

ARTICLE INFO

Keywords:
Electrospinning
Nanofibers
Multivalent batteries
Cathodes

ABSTRACT

Electrospinning is a remarkably versatile and cost-effective technique known for its simplicity and flexibility in manufacturing porous fibers with an expansive surface area. This technique's flexibility enables the creation of nanofibers with diverse structures and scaffolds. These nanofibers are sometimes subjected to heat treatments before being applied. Their unique characteristics render them exceptionally suitable for integration into energy storage systems. In the realm of energy storage systems like batteries, a pressing demand exists for alternatives beyond lithium-ion batteries. Multivalent batteries, such as Al-ion, Mg-ion, Zn-ion, and Ca-ion batteries, thanks to their advantageous characteristics, represent a suitable choice. Due to their porous nature, electrospun fibers facilitate ion transfer, enhance charge/discharge processes, and improve battery kinetics. In this paper, we will examine into how electrospun fibers are used in multivalent battery cathodes and unveil the extra advantages they offer to these battery systems. Finally, a comprehensive evaluation will be conducted to assess this technique's both the advantages and challenges. Prospects for high-capacity batteries, specifically calcium-ion batteries, will also be considered.

1. Introduction

As the development of renewable energy sources such as solar and wind energy progresses rapidly, the demand for affordable, safe, and cyclically stable energy storage batteries grows [1–5]. While lithium-ion batteries offer high energy density, long lifespan, broad operating temperature ranges, and low self-discharge rates [1,3,6–8], their limited lithium reserves, uneven distribution, and high cost pose challenges [1,8,9]. Therefore, there is a need to explore alternative electrochemical energy storage technologies that utilize abundant natural elements with properties similar to lithium [1,6], such as Magnesium, Zinc, Calcium, and Aluminum. Abundant in the Earth's crust, these elements contribute to the production of cost-effective batteries. Their multivalency and ability to transfer 2 or 3 electrons in redox reactions result in a higher energy density. Additionally, characteristics such as extended lifespan and enhanced safety have generated significant interest in electrochemical energy storage systems [3,4,6,9–15]. However, a significant challenge arises from the intricate electrostatic interactions among multivalent ions. These interactions have several adverse effects, such as impeding solid-state diffusion kinetics [14,16–18], delaying ion diffusion [4,9,19], inducing polarization within the host environment, and potentially compromising the rate capability of these battery systems. Consequently, a significant hurdle in advancing multivalent battery technology lies in identifying electrode materials capable of reversibly efficiently inserting and extracting multivalent cations [20]. This quest is vital for maintaining optimal charge-discharge efficiency and ensuring long-term cycle life [21] while addressing the issue of pronounced polarization caused by polyvalent ions [22]. Notably, the cathode emerges as a critical component, holding the potential to alleviate many of these challenges and significantly influencing the performance of multivalent metal-ion batteries [14]. The electrospinning technique offers a viable solution for addressing the challenges associated with multivalent battery cathodes.

Electrospinning is highly advantageous, scalable, and cost-effective method for producing remarkably fine polymer fibers with high surface area, exceptional mechanical attributes, and conductivity. It has diverse uses across a range of industries, including biotechnology [23–28], filtration membranes [29–31], catalysis [32–34], and energy storage systems [35–43]. Electrospun mats have captured considerable interest in the field of energy storage systems like batteries due to their unique characteristics, such as a porous structure, short ion diffusion path, and a large surface area. Consequently, numerous researchers have

* Corresponding authors.
E-mail addresses: baharzare@sharif.edu (B. Zare), sadrnezh@sharif.edu (S.K. Sadrnezhaad).

https://doi.org/10.1016/j.est.2024.110514
Received 5 November 2023; Received in revised form 19 December 2023; Accepted 6 January 2024
Available online 17 January 2024
2352-152X/© 2024 Elsevier Ltd. All rights reserved.

been drawn to explore the manifold possibilities of utilizing these mats in various battery components, including electrodes [44–46], electrolytes [47–49], and separators [49].

Electrospinning is a method used to produce fibers in a range of nano to micro, involving three main components: such as a syringe with a metal needle, a high-voltage power supply, and a conductive collector, as schematically shown in Fig. 1. Electrostatic repulsion overcomes the surface tension of the solution, leading to the formation of a conical drop known as the Taylor cone at the tip of the needle. This effect creates of a charged fine jet propelling the polymer solution toward the collector. The interaction between the electric field and the solution's surface tension causes the jet to stretch and undergo whipping motions, leading to solvent evaporation and continuous jet elongation into a long, thin fiber. The fibers then solidify, forming a uniform fiber mat. The properties of electrospun nanofibers are influenced by a range of parameters, with these factors playing a crucial role in determining the morphology and diameter of the fibers during the electrospinning process:

- **Solution parameters**: These include the solution's concentration or viscosity, the molecular weight of the polymers used, surface tension, and electrical conductivity.
- **Process parameters**: These encompass the feeding rate, applied voltage, distance between the syringe and collector, and needle diameter.
- **Ambient conditions**: Factors like temperature and the environment also play a role [50–55].

So, the application of versatile electrospinning techniques shows great promise in enhancing the reliability of cathodes in multivalent batteries. This review exclusively focuses on research conducted from 2019 to 2023, emphasizing the potential of electrospun cathodes in multivalent batteries and highlighting their unique performance. The primary emphasis is on addressing challenges such as low ion diffusion kinetics, specific capacity, and cyclability. Through the analysis of electrospun fiber architecture, it unveils crucial insights into their structural and morphological features, essential for comprehending their behavior in battery applications. Moreover, the work surpasses conventional approaches by integrating advanced characterization techniques, including electron microscopy and spectroscopy. This integration allows the authors to offer a comprehensive review of the physical and chemical properties of fibers. By elucidating the intricate interplay between fiber structure and electrochemical performance, the research not only contributes to the fundamental understanding of electrospun fibers but also pioneers their application in next-generation energy storage systems, thereby making significant strides in the field. The assessment begins with an analysis of metal sulfides and extends to metal nitrides, metal selenides, and metal oxides. Through this comprehensive exploration, the authors aim to shed light on the broader landscape of electrospun cathodes, paving the way for advancements in energy storage technologies.

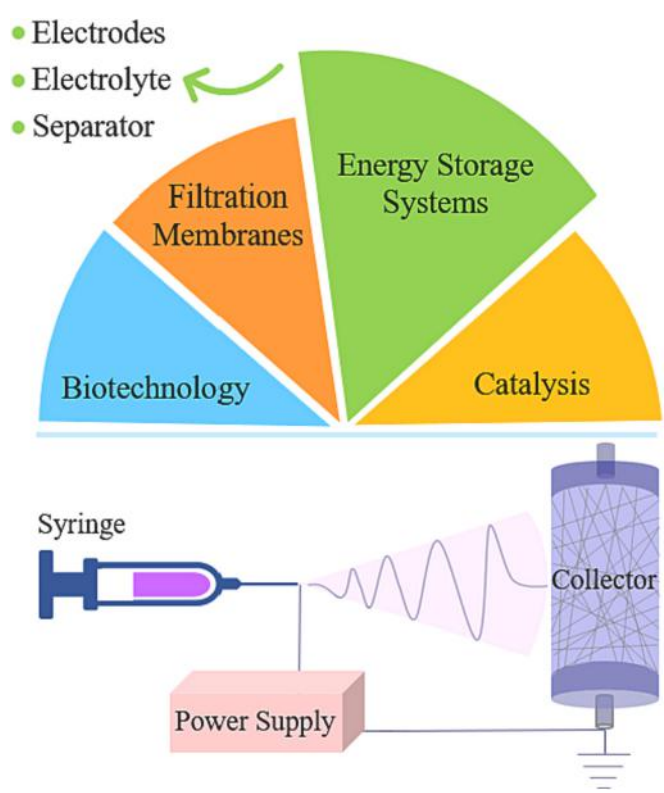

Fig. 1. Application of electrospinning technique and a schematic of fundamental electrospinning setup.

2. Application of electrospun cathodes in multivalent batteries

2.1. Metalsulfides

2.1.1. Molybdenum (IV) sulfide (MoS_2)

Energy storage systems, especially batteries, require high-performance materials. MoS_2 is widely embraced due to its features, such as electronic properties and a layered structure, which facilitate the incorporation of external substances with relative ease, alongside its impressive capacity [56–59]. However, MoS_2 faces challenges such as poor electrical conductivity and structural instability. Incorporating MoS_2 within a carbon framework has proven to be a viable solution to overcome these limitations. This composite structure provides excellent stability and optimizes the cyclability of charge and discharge by facilitating easier ion and electron transfer. In a study conducted in 2019, Yang et al. [57] successfully employed MoS_2 as a cathode material in aluminum-ion batteries. To enhance performance and address restrictions, as schematically illustrated in Fig. 2A(a), researchers synthesized a binder-free cathode named MoS_2@CNFs, based on MoS_2 and carbon nanofibers (CNFs). They achieved this synthesis using electrospinning and annealing techniques, effectively preventing unwanted reactions between the electrolyte and the cathode. These fabricated fibers display uniformity and continuity, featuring a 3D porous structure as depicted in Fig. 2A(b, c). The battery cell combined the MoS_2@CNFs cathode, aluminum foil anode, and [EMIm]Cl + $AlCl_3$ electrolyte. The initial discharge capacity at 100 mA g^{-1} was 293.2 mAh g^{-1}, slightly decreasing to 126.6 mAh g^{-1} after 200 cycles. These findings underscore the exceptional cyclability and capacity of MoS_2@CNFs-based aluminum-ion batteries, attributed to their meticulously crafted and unique structure. Furthermore, the outstanding electrochemical performance of MoS_2@CNFs in these batteries, along with the intercalation and deintercalation of Al^{3+} ions during charge and discharge cycles between the layers of MoS_2, has been identified through ex situ XRD (Fig. 2A(d)) and XPS analysis (Fig. 2A(e)). Incorporating MoS_2 within a carbon framework addresses the challenges of poor electrical conductivity and structural instability. It enhances the overall performance of aluminum-ion batteries, making them a promising candidate for next-generation energy storage systems [57].

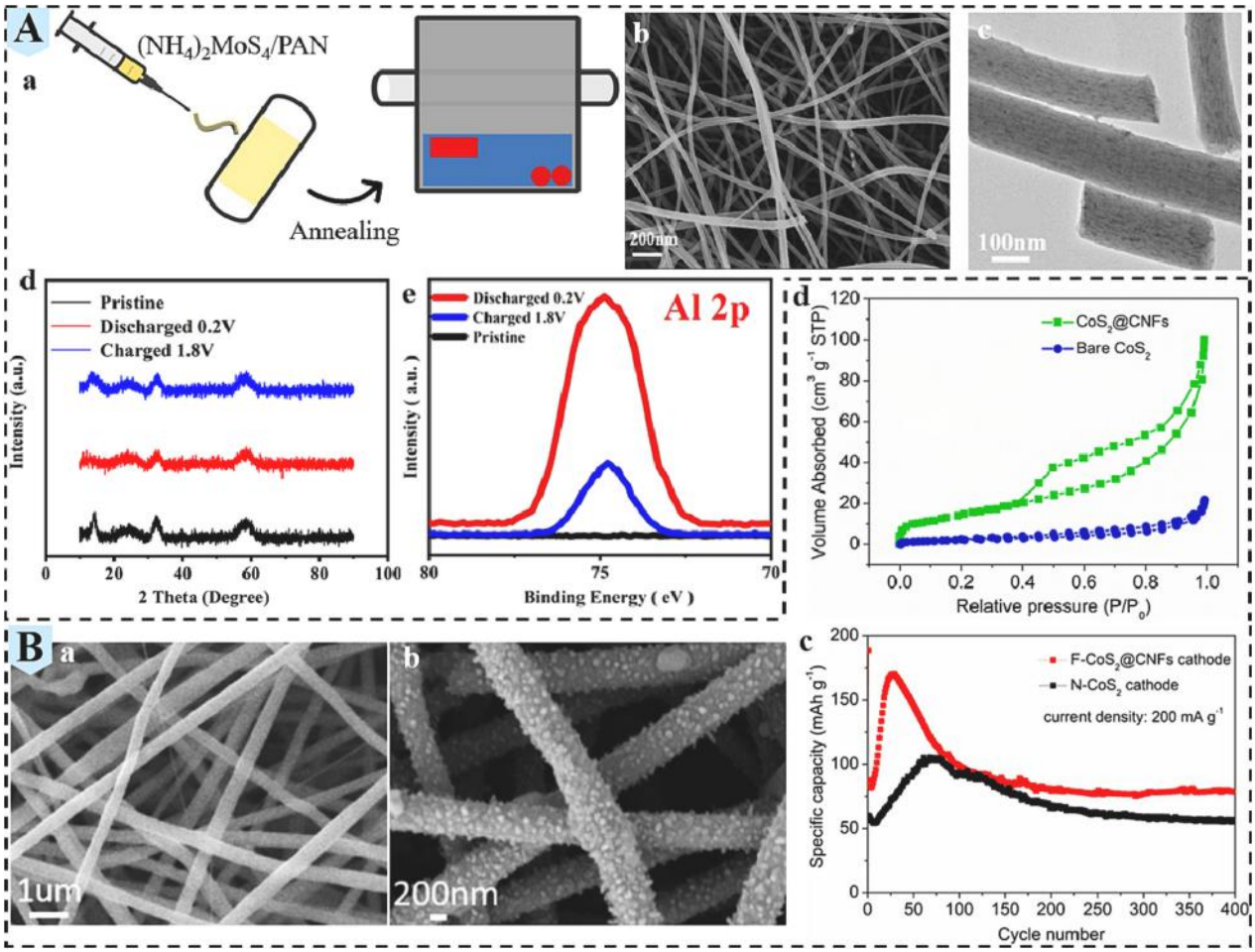

Fig. 2. A. Illustration of the MoS_2@CNFs; a) Schematic of the MoS_2@CNFs fabrication process; b) SEM image of MoS_2@CNFs; c) TEM image of MoS_2@CNFs; d) Ex situ XRD patterns of the MoS_2/CNFs cathode; e) XPS data of the Al 2p peak of the MoS_2/CNFs cathode: pristine, fully charged (1.8 V), and fully discharged (0.2 V); Adapted with permission. [57] Copyright 2019, American Chemical Society. B. Illustration of the CoS_2@CNFs; a–b) SEM image of CoS_2@CNFs; c) Cycling performance of typical cathode as N-CoS_2 and binder-free cathode as F-CoS_2@CNFs-C at 200 mA g^{-1}; d) Nitrogen adsorption-desorption isotherms of bare CoS_2 and CoS_2@CNFs; Adapted with permission. [60] Copyright 2021, Elsevier.

2.1.2. Cobalt (II) sulfide (CoS_2)

Cobalt sulfides stand out for their electrical and catalytic properties, substantial surface area, and impressive theoretical capacity, rendering them promising for battery and supercapacitor applications [60–64]. In a significant development in 2021, Zhuang et al. [60] explored using of CoS_2 as a cathode material in aluminum-ion batteries. A CoS_2@CNF nanostructure was synthesized via electrospinning and annealing to create a binder-free cathode. Its performance was compared to a conventional CoS_2 cathode with a binder. Based on Fig. 2B(a, b), the uniform distribution and small particle size of CoS_2 particles on the carbon matrix reduce ion diffusion distance. The composite nanofibers used as a cathode form a 3D electron conductive transport network with high specific surface area, simplifying ion diffusion, enabling efficient electrochemical reactions, and enhancing electrolyte penetration. The battery cell consisted of a CoS_2@CNFs cathode, a high-purity aluminum foil anode, and [EMIm]Cl + $AlCl_3$ electrolyte. Fig. 2B(c) depicts that the CoS_2@CNFs cathode exhibited superior cycling stability and rate capacity compared to the conventional CoS_2 cathode, maintaining a specific capacity of 82 mAh g^{-1} after 400 cycles at a current density of 200 mA g^{-1}. In contrast, the conventional CoS_2 cathode retained a specific capacity of 55 mAh g^{-1} under the same conditions. This improved performance of the CoS_2@CNFs cathode can be attributed to the absence of a binder, which prevents electrolyte-binder reactions. Additionally, as revealed in Fig. 2B(d), Brunauer–Emmett–Teller (BET) analysis and N_2 adsorption/desorption isotherms were employed to elucidate the pore structures of CoS_2 and CoS_2@CNFs. The specific surface areas of pure CoS_2 and CoS_2@CNFs were determined to be 13.42 and 123.63 m^2 g^{-1}, respectively. Clearly, the composites exhibited a significantly larger specific surface area. To further discern the distribution of pore sizes, Barrett-Joyner-Halenda (BJH) method was conducted. In addition to the positive aspects of these cathodes, a challenge arises in the reduced capacity during the initial cycles. This decrease may be attributed to the formation of a solid electrolyte interphase (SEI), potentially resulting from excessive contact between the electrode and electrolyte. Furthermore, when compared to the electrode in the charging phase, the electrode in the discharge phase exhibits a more pronounced peak for Al 2p, as revealed by ex situ XPS analysis. Additionally, EDS mapping results show a weaker signal in the discharge phase, highlighting the persistent presence of Al^{3+} concentration. These phenomena can be traced back to the irreversible insertion of Al species [60].

2.1.3. Nickel disulfide (NiS_2)

NiS_2 showcases noteworthy features, including beneficial electrical conductivity, anion redox capability, high theoretical capacity, and abundant resources [65,66]. Consequently, utilizing NiS_2 as a cathode material in aluminum-ion batteries is an effective strategy for enhancing reliable cycling durability and reversible capacity. In a recent research study performed by Li et al. [65] in 2022, a cathode electrode known as NiS_2/SC@SCNF (NiS_2/S-doped carbon@S-doped carbon nanofiber) was developed using a multi-step process involving electrospinning,

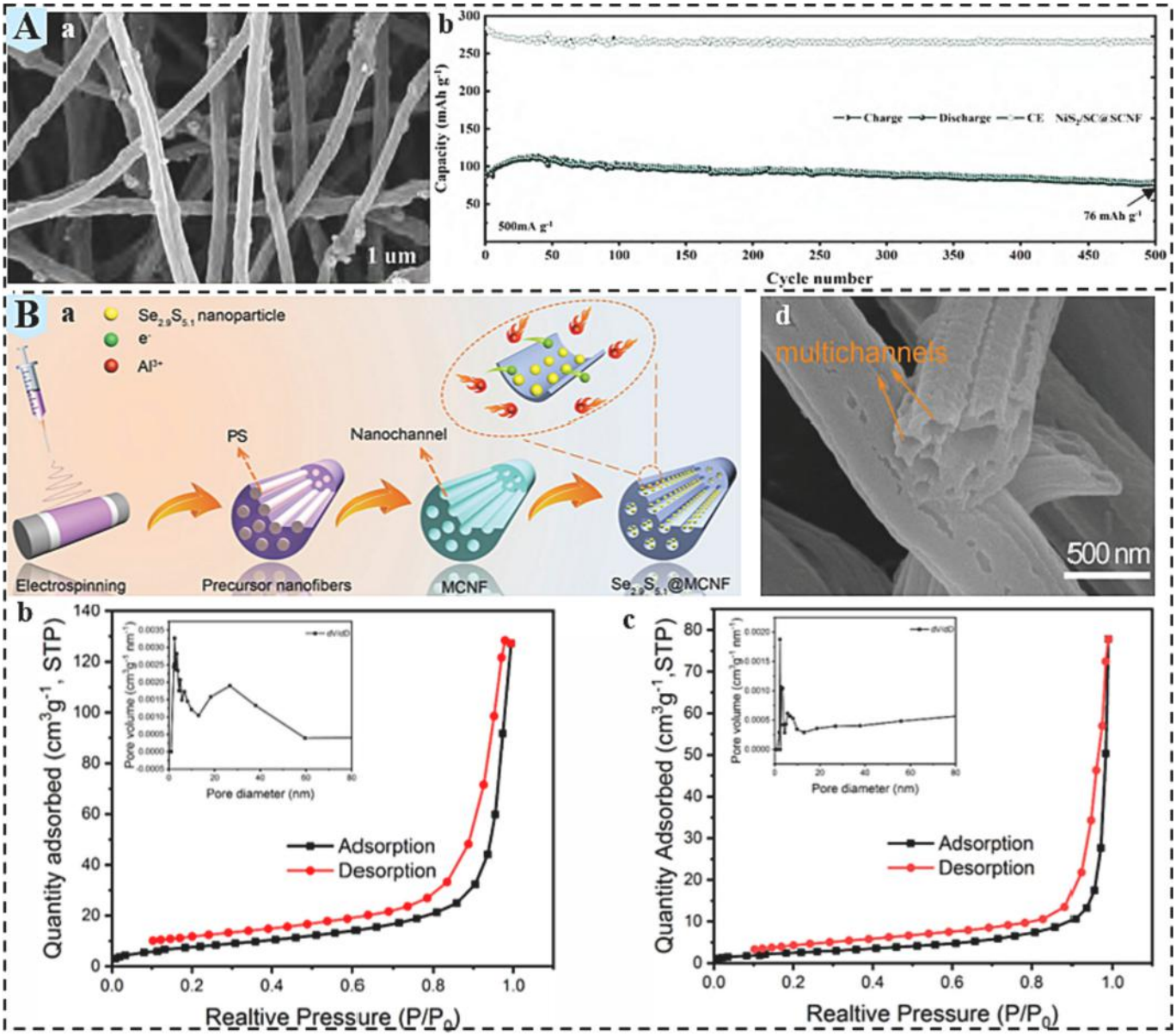

Fig. 3. A. Illustration of the NiS_2/SC@SCNF; SEM images of a) NiS_2/SC@SCNF; b) Long-cycling performance of NiS_2/SC@SCNF material at 500 mA g^{-1}; Adapted with permission. [65] Copyright 2022, Elsevier. B. Illustration of the $Se_{2.9}S_{5.1}$@MCNF; a) Schematic the synthesis of $Se_{2.9}S_{5.1}$@MCNF; The N_2 adsorption-desorption isotherms and the associated pore size distribution curve for b) $Se_{2.9}S_{5.1}$@MCNF and c) pristine MCNF; d) FE-SEM images of $Se_{2.9}S_{5.1}$@MCNF; Adapted with permission. [67] Copyright 2022, Wiley-VCH GmbH.

pyrolysis, and sulfidation. As represented in Fig. 3A(a), it resulted in the formation of a 3D electrical conductivity network of SCNF, facilitating efficient electron transfer, optimizing the NiS_2/SC conductivity, and preventing the dissolution of polysulfide ions in the electrolyte and their subsequent reactions. As a result, NiS_2/SC@SCNF exhibits improved electrochemical performance and exceptional cyclability. A cathode comprising NiS_2/SC@SCNF, an anode made of metallic aluminum, and an electrolyte of [EMIm]Cl + $AlCl_3$ were integrated to constructing a battery cell. This battery demonstrates a consistent capacity of 82 mAh g^{-1} at a current density of 200 mA g^{-1} after 100 cycles and 76 mAh g^{-1} at 500 mA g^{-1} after 500 cycles (Fig. 3A(b)), highlighting the promising potential of NiS_2-based cathodes in aluminum-ion batteries [65].

2.1.4. Selenium sulfide (Se_xS_y)

Selenium-sulfur (Se—S) cathodes demonstrate outstanding electrochemical performance due to selenium's high electrical conductivity and sulfur's high capacity [67–70]. Elements such as selenium and sulfur are utilized to enhance the capabilities of aluminum-ion batteries because of their high theoretical capacity and energy density. In 2022, Li et al. [67] developed Se—S nanofibers and a multichannel carbon structure known as $Se_{2.9}S_{5.1}$@MCNF with the electrospinning technique and calcination, as shown in Fig. 3B(a). The $Se_{2.9}S_{5.1}$@MCNF cathode maintains its structural integrity even after long-term cycles and, being binder-free, prevents cathode-electrolyte reactions. As depicted in Fig. 3B(b, c), N_2 adsorption/desorption isotherms, porosity parameters, specific surface area, and pore size distribution of $Se_{2.}9S_{5.1}$@MCNF and MCNF were analysed. BET specific surface area of $Se_{2.9}S_{5.1}$@MCNF (10.06 m^2 g^{-1}) was observed to be lower compared to the MCNF host (39.27 m^2 g^{-1}). This suggests that a significant portion of $Se_{2.}9S_{5.1}$ molecules successfully integrated into the MCNF structure, and the XRD pattern and characteristic peaks reveal the uniform distribution of $Se_{2.9}S_{5.1}$ within the MCNF host. Additionally, $Se_{2.9}S_{5.1}$@MCNF exhibited mesopores of 2.32 nm (2.34 nm for MCNF), which can effectively facilitate electrolyte accessibility. The multichannel network (Fig. 3B(d)) provides

mechanical support and stable conductivity, enhancing electron and ion diffusion rates while minimizing solubility and volume expansion. A battery cell was assembled by combining a cathode composed of $Se_{2.9}S_{5.1}$@MCNF, an anode made of high-purity aluminum foil, and an electrolyte comprising [EMIm]Cl + $AlCl_3$. In contrast to other electrodes (SeS@MCNF and SeS_2@MCNF), which exhibit a limited specific capacity of 100 mAh g^{-1} under a current density of 50 mA g^{-1}, the $Se_{2.9}S_{5.1}$@MCNF electrode demonstrates a discharge capacity of up to 606 mAh g^{-1} under the same current density. It maintains a capacity of 187 mAh g^{-1} at 500 mA g^{-1} even after 3000 cycles. These results highlight its strong stability attributed to the optimized selenium/sulfur ratio and advanced multichannel structure [67].

2.2. Metal nitrides

2.2.1. Vanadium nitride (VN)

Vanadium-based materials, characterized by diverse oxidation states, compositions, and structures, have demonstrated notable attributes, such as prolonged cyclability and high reversible capacity [71–73]. Nonetheless, their electrical conductivity is often limited, and they suffer from an unstable structure [71,74]. To surmount these challenges, Zhang et al. [71], in 2022, investigated the potential of vanadium nitride (VN) owing to its exceptional electrical and ionic conductivity [71,75], making it a promising candidate for battery applications. Their pioneering approach involved fabrication 3D carbon nanofiber composites enriched with nitrogen, known as VN/N-CNF. These composites have a specific surface area of 37.2 m^2 g^{-1} and a pore size distribution in the range of 1–10 nm. They serve as a binder-free cathode material in zinc-ion batteries. This achievement was accomplished through the synergistic employment of electrospinning and thermal treatment techniques, as schematically illustrated in Fig. 4 (a). Electrospinning facilitated the construction of a flexible and intact 3D framework for VN/N-CNF (Fig. 4(b, c)). At the same time, incorporating nanofibers as a conductive matrix improved electrical conductivity. Additionally, this distinctive architecture effectively mitigated vanadium dissolution and minimized direct contact with the electrolyte, improving stability. The battery configuration consisted of the VN/N-CNF cathode, a zinc plate as the anode, and $Zn(CF_3SO_3)_2$ as the electrolyte. As outlined in Fig. 4(d), the battery exhibited outstanding cyclability, maintaining a reversible capacity of 482 mAh g^{-1} out of a maximum capacity of 50,000 mA g^{-1} after 30,000 charge-discharge cycles. Furthermore, it demonstrated an exceptional capability with a discharge capacity of 297 mAh g^{-1} at an extremely high rate of 100,000 mA g^{-1}. These results highlight the impressive performance of the VN/N-CNF composite as a cathode material, showcasing its potential for future battery applications [71].

2.3. Metal selenides

2.3.1. Molybdenum diselenide ($MoSe_2$)

$MoSe_2$ has a layered structure and a substantial surface area, allowing for ion's rapid movement. Moreover, it boasts a high theoretical capacity. These inherent attributes have made it a valuable choice for battery systems [76–79]. However, inherent issues with layered transition metal dichalcogenides (TMDs), such as weak conductivity and volume fluctuations during the charge/discharge process, contribute to insufficient longevity and limited cyclability. To address these challenges, $MoSe_2$ is often combined with a conductive substrate, such as carbon material [80]. In a noteworthy study executed in 2020 by Yang et al. [81], a cathode for aluminum-ion batteries was synthesized using a combination of electrospinning, annealing, and hydrothermal reaction processes, yielding the formation of N-doped carbon nanofibers and $MoSe_2$ as $MoSe_2$@NCNFs. The resulting aluminum-ion battery configuration comprised a $MoSe_2$@NCNF cathode, a high-purity Al foil as the anode, and [EMIm]Cl + $AlCl_3$ as the electrolyte. By incorporating NCNFs into the composite architecture, a 3D matrix endowed with exceptional conductivity and flexibility was achieved (Fig. 5A(a)), facilitating the efficient transport of ions and electrons. In addition, the introduction of nitrogen doping profoundly augmented the electrical conductivity of carbon nanofibers. As shown in Fig. 5A(b), The $MoSe_2$@NCNF composite demonstrated an impressive initial discharge capacity of 296.3 mAh g^{-1} at a current density of 100 mA g^{-1}. Remarkably, even after 200 charge/discharge cycles, the composite maintained a sustained discharge capacity of 169.9 mAh g^{-1} with negligible fading. The intercalation and deintercalation processes of Al^{3+} ions in the interlayer of the $MoSe_2$ network during charge and discharge, respectively, have also been investigated. This is outlined in Fig. 5A(c) using ex situ XRD. In some cases, the reason for not returning to the initial state is the trapping of Al^{3+} ions in the $MoSe_2$ lattice due to the presence of the solid electrolyte interface (SEI). These findings

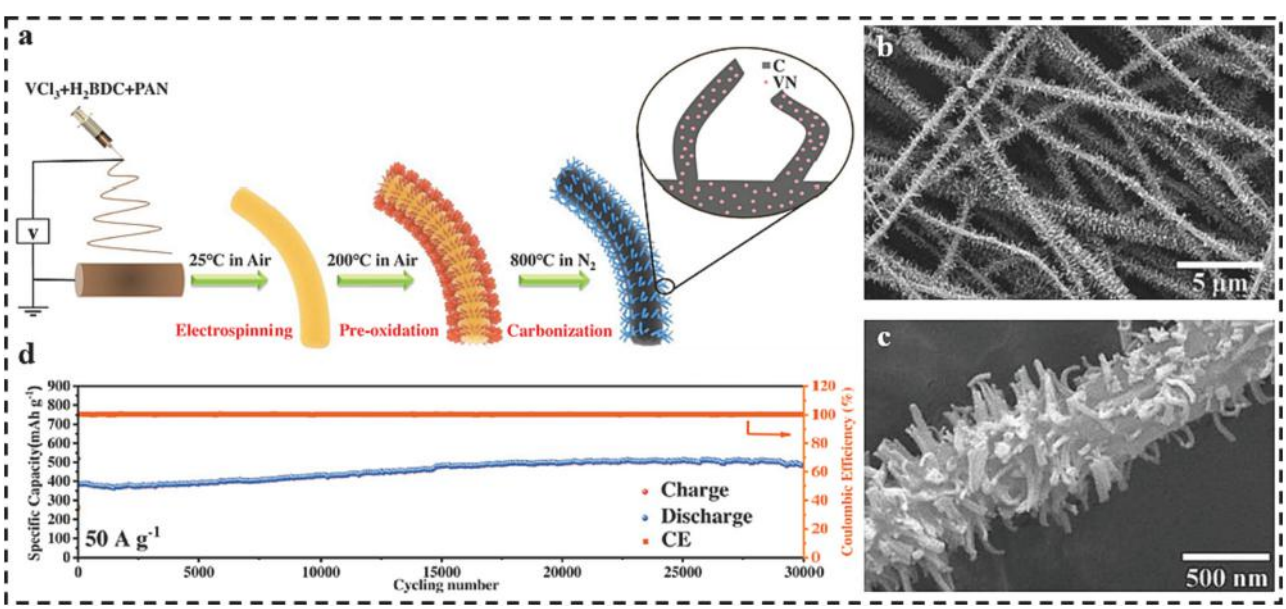

Fig. 4. Illustration of the VN/N-CNF; a) Schematic illustration of the synthesis of VN/N-CNF; b, c) Low-magnification and high-magnification FESEM images of VN/N-CNFs, respectively; d) Long-term cycling performance of VN/N-CNFs at 50000 mA g^{-1}; Adapted with permission. [71] Copyright 2022, Wiley-VCH GmbH.

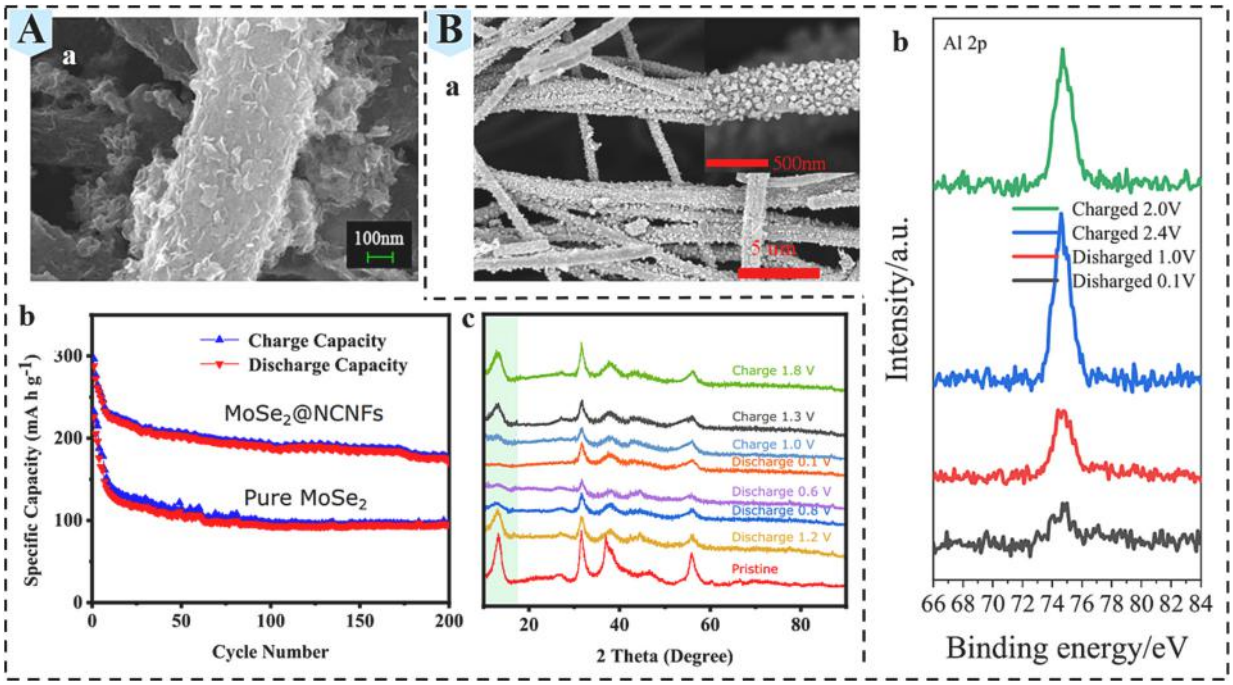

Fig. 5. A. Illustration of the MoS_2@CNFs; SEM images of a) $MoSe_2$@NCNF; b) Long-term cycling stability test at a current density of 100 mA g^{-1} for pure $MoSe_2$ and $MoSe_2$@NCNF; c) Ex-XRD patterns of the $MoSe_2$@NCNF cathode at various charge and discharge states; Adapted with permission. [81] Copyright 2020, Springer-Verlag GmbH Germany, part of Springer Nature. B. Illustration of the $Cu_{1.8}Se$ carbon nanofiber composite; a) SEM images of Cu-based fibers; b) XPS pattern of $Cu_{1.8}Se$-1000 (The selenization temperature is 1000 °C) (Al 2p) during charge/discharge process; Adapted with permission. [88] Copyright 2023, Elsevier.

underscore the compelling potential of the $MoSe_2$@NCNF composite as a binder-free cathode material for aluminum-ion batteries, characterized by outstanding electrochemical performance, superior rate capability, high specific capacity, and exceptional cyclic stability [81].

2.3.2. Copper (II) selenide (CuSe)

CuSe has notable characteristics in battery research, including substantial specific capacity, long-term stability, and economic viability, as evidenced by numerous studies [82–86]. To further enhance the electrochemical performance of CuSe, combining its properties with carbon materials emerges as a wise strategy [87]. On the other hand, carbon-based cathodes, featuring ample pore dimensions and an expansive surface area, exhibited favorable characteristics that enhance ion transport and long-term cycling stability [88]. In 2023, Zhang et al. [88] pioneered the development of a cathode for aluminum-ion batteries. They employed a $Cu_{1.8}Se$ carbon nanofiber composite, synthesized through electrospinning and high-temperature (600 °C, 800 °C, 1000 °C) selenization processes. As revealed in Fig. 5B(a), the resulting 3D-structured, binder-free cathode facilitates ion diffusion and enables efficient electron transmission, ultimately leading to an increased specific capacity for the material. The battery configuration included a pure Al foil as the anode and the $Cu_{1.8}Se$ carbon nanofiber composite as the cathode. After 5000 cycles, the researchers reported a specific discharge capacity of approximately 152 mAh g^{-1} at a current density of 2000 mA g^{-1}. Apart from electrochemical tests, XPS, BET, and X-ray diffraction were also conducted. XPS was employed to investigate the cathode mechanism during the charge and discharge of the electrochemical reaction (Fig. 5B(b)). BET results provided valuable insights into $Cu_{1.8}Se$-1000, revealing an average pore size of approximately 0.85 nm and a specific surface area of 139.12 m^2 g^{-1}. This composition features the smallest grain size and a high specific surface area, significantly enhancing its electrochemical performance. XRD analysis demonstrated the highest crystallinity for $Cu_{1.8}Se$-1000, indicating a notable proportion of crystalline areas and the smallest grain size. These tests underscore the importance of improving the connection between materials and the electrolyte, facilitating the intercalation/deintercalation of ions and providing more sites for redox reactions. Generally, the battery exhibited notable electrochemical performance, highlighting the potential of exploring cathodes comprising mediator metals and selenide-based materials as a novel research direction [88].

2.4. Metal oxides

2.4.1. Manganese oxides

Manganese oxides have numerous advantages, such as low toxicity, cost-effectiveness, diverse crystal structures, and high energy density, making them promising candidates for battery applications. However, their weak electrical conductivity, manganese dissolution tendency, and low structural stability result in poor capacity and subpar electrochemical performance [89–95]. To address these challenges, coating the manganese oxides with carbon-based materials can effectively prevent structural disintegration, leading to improved electrochemical performance [91].

2.4.1.1. Manganese (II,III) oxide (Mn_3O_4). In a research study conducted in 2020 by Long et al. [89], they incorporated manganese (II, III) oxide (Mn_3O_4) nanoparticles into hollow carbon fibers, resulting in the formation of Mn_3O_4@HCFs (Fig. 6A(a)). These composite materials served as the cathode in Zinc-ion batteries. While Mn_3O_4 boasts an attractive theoretical capacity and high theoretical voltage, it faces challenges, including poor electrical conductivity, limited cyclability, and reduced discharge capacity caused by volume fluctuations [96–98]. Various conductive materials were incorporated to address these issues and enhance electrical conductivity. Co-axial electrospinning and carbonization techniques were used to synthesize Mn_3O_4@HCFs. Carbon nanofibers have become prominent in electrode materials due to their ability to enhance ion and electron transport, excellent electrical conductivity, and a large specific surface area, as demonstrated in Fig. 6A(b) by the BET test. For instance, Mn_3O_4@HCFs-7.5 exhibits a specific surface area of 37.85 m^2 g^{-1}. Furthermore, the carbon shell

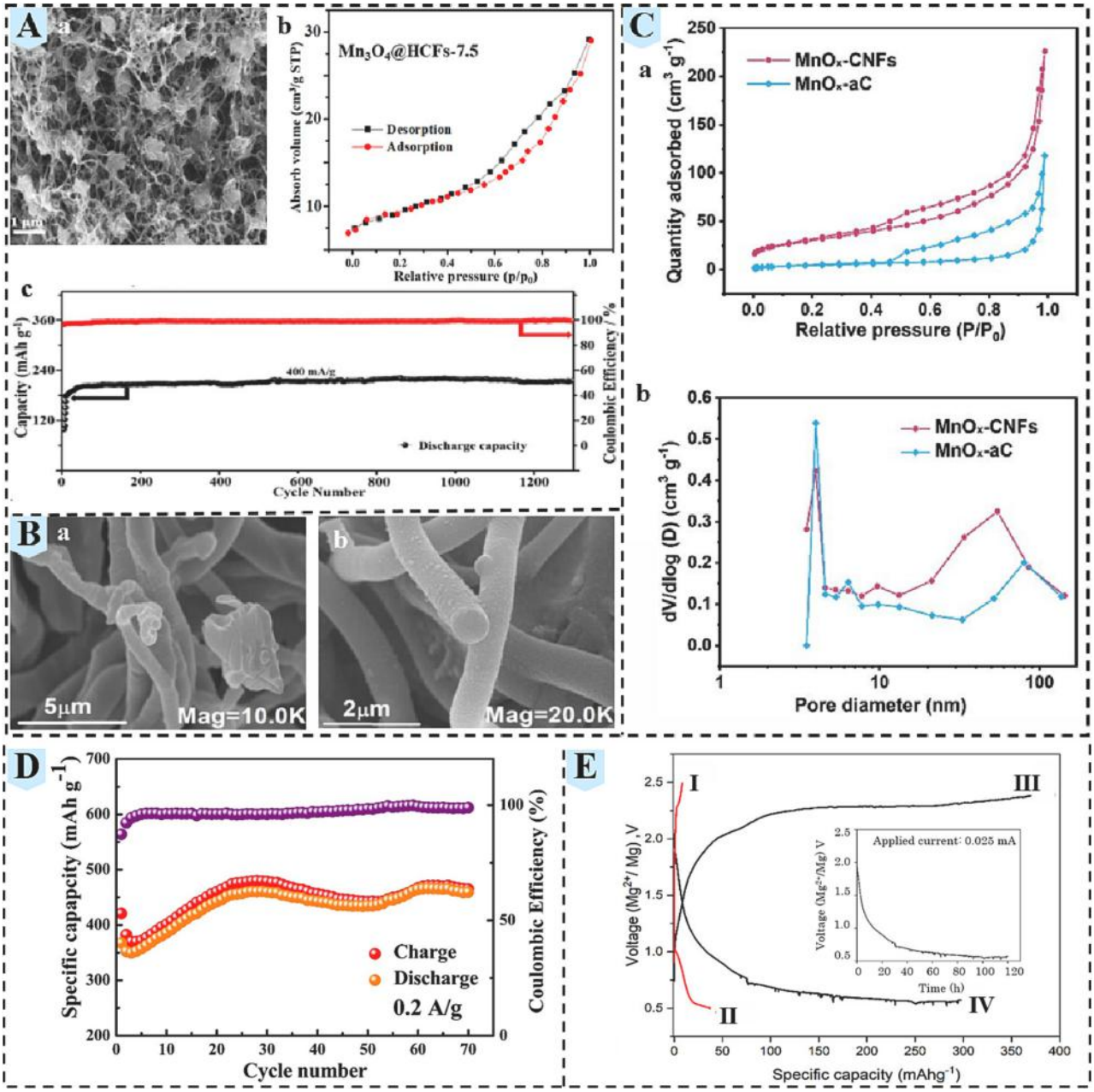

Fig. 6. A. Illustration of the Mn_3O_4@HCFs; a) FESEM image of the Mn_3O_4@HCFs-7.5 (7.5 is the percentage of PAN in electrospinning solution); b) Nitrogen adsorption/desorption isotherms of the Mn_3O_4@HCFs-7.5; c) Cycling performance and Coulombic efficiency of Mn_3O_4@HCFs-7.5 electrode at 400 mA g^{-1}; Adapted with permission. [89] Copyright 2020, Elsevier. B. Illustration of the MnO@N-C; SEM image of a) the precursor and b) MnO@N-C-500 (The annealing temperature is 500 °C); Adapted with permission. [90] Copyright 2020, Elsevier. C. Illustration of the MnOx-CNFs; a) N_2 adsorption-desorption isotherms of MnO_x-CNFs and MnO_x-aC; b) The pore size distribution of MnO_x-CNFs and MnO_x-aC; Adapted with permission. [91] Copyright 2022, American Chemical Society. D. Illustration of the Mn_2O_3@CNFs; a) Cycling stability of F-500 (The annealing temperature is 500 °C) at a rate of 200 mA g^{-1}; Adapted with permission. [92] Copyright 2022, Elsevier. E. Illustration of the $MgMn_2O_4$; Typical initial galvanostatic charge-discharge curves of $MgMn_2O_4$; (I) and (II) before electrospinning, (III) and (IV) after electrospinning; Adapted with permission. [99] Copyright, Taylor & Francis.

minimizes the dissolution of the manganese structure during charge/discharge cycling within this cathode. The Zn-ion battery was assembled using zinc foil as the anode, Mn_3O_4@HCFs as the cathode, and $ZnSO_4$ + $MnSO_4$ as the electrolyte. The battery demonstrated remarkable capabilities by utilizing porous HCFs to enhance cyclability and specific capacity, and with the core-shell structure of Mn_3O_4@HCFs featuring numerous gaps leading to outstanding electrochemical performance. The experimental results demonstrated discharge capacities of 215.8 mAh g^{-1} and 115.7 mAh g^{-1} at a current density of 300 mA g^{-1} and 2000 mA g^{-1}, respectively. The battery exhibited impressive cycling stability at 400 mA g^{-1} after 1300 cycles, as shown in Fig. 6A(c). Consequently, this research showcases a stable and cost-effective solution for energy storage systems [89].

2.4.1.2. Manganese (II) oxide (MnO). In 2020, Tang et al. [90] researched to develop a cathode material for Zn-ion batteries. This research involved the synthesizing a MnO@N-C composite through electrospinning and a two-step annealing process. The incorporation of carbon in MnO@N-C composite not only enhances electrical conductivity but also significantly improves its electrochemical performance. As shown in Fig. 6B(a, b), the composite structure evenly distributed

MnO nanoparticles within a porous carbon matrix, facilitating ion diffusion. This arrangement increases the surface area of MnO, ultimately enhancing the rate capability even under high current densities. Moreover, ex situ XRD analysis was conducted, revealing no structural collapse of manganese (Mn) during the energy storage process. A battery was constructed with zinc foil employed as the anode, MnO@N-C as the cathode, and $ZnSO_4$ as the electrolyte to evaluate the potential of the MnO@N-C composite. Reversibly, the battery exhibited a capacity of 176.3 mAh g^{-1} under a current density of 500 mA g^{-1} after undergoing 200 cycles. The MnO@N-C composite's positive cyclability performance and superior rate capability underscore its potential for extensive utilization in battery technology. Furthermore, although this cathode showed some degree of self-discharge, it offers an appealing combination of affordability and environmental compatibility, making it an attractive choice for various battery systems [90].

2.4.1.3. Manganese (x) oxide (MnO_x). In a 2022 study, Ding et al. [91] successfully synthesized manganese oxide coated with carbon nanofibers (MnO_x-CNFs) using the electrospinning technique. The binder-free cathode, composed of one-dimensional CNFs, exhibited exceptional electrical conductivity and superior electrochemical kinetics compared to other carbon matrices. The porous structure of MnO_x-CNFs was investigated using N_2 adsorption/desorption isotherms. The results reveal a predominantly mesoporous structure with a specific surface area of 108.1 m^2 g^{-1}. For comparison, based on the depiction in Fig. 6C (a, b), MnO_x-aC (MnO_x and an amorphous carbon composite, MnO_x-aC, without CNFs coating) was also analysed and exhibited a specific surface area of 16.3 m^2 g^{-1}. Therefore, the MnO_x-CNFs possess a significantly larger specific surface area and mesoporous structure, which can facilitate effective electrolyte diffusion and accommodate volume expansion during the charge/discharge process. Additionally, this carbon coating prevents manganese dissolution, enhances load transfer, and shortens ion and electrode diffusion pathways. The assembled battery consisted of a zinc foil anode, the MnO_x-CNFs cathode, and a $ZnSO_4$ + $MnSO_4$ electrolyte. Remarkably, this battery demonstrated a high specific capacity of 220 mAh g^{-1} at a current density of 1000 mA g^{-1}.

Moreover, it exhibited excellent cyclability, with a remarkable 71 % capacity retention at 3000 mA g^{-1} after 5000 cycles. The remarkable rate performance and cyclability exhibited by MnO_x-CNFs outperformed the majority of Mn-based cathodes, establishing them as exceptional materials for Zn-ion batteries. This advancement paved the way for developing Zn-ion batteries with significantly increased capacity, and extending their cycle life, making them ideal for energy storage systems [91].

2.4.1.4. Manganese (III) oxide (Mn_2O_3). Among Manganese-based oxides, Mn_2O_3 stands out, despite its subpar cycling performance and inevitable volume fluctuations. Nonetheless, it offers a more straightforward synthesis process and boasts a superior specific theoretical capacity compared to MnO_2 and Mn_3O_4. In 2022, Cheng et al. performed a study [92] that delved deeper into this topic. They fabricated a 3D Mn_2O_3 nanofiber using electrospinning and annealing. This nanofiber was purposefully designed as a cathode for Zn-ion batteries. The battery assembly included Mn_2O_3 as the cathode, high-purity zinc foil as the anode, and a hydrogel electrolyte. The cycling performance with a current density of 200 mA g^{-1} in the Mn_2O_3 cathodes is depicted in Fig. 6D. Impressively, after subjecting the battery to 1000 cycles, it achieved an outstanding capacity of 104 mAh g^{-1} at a rate of 2000 mA g^{-1}. Notably, electrospinning offers several advantages, including improved cathode-electrolyte contact, enhanced electrical conductivity due to the presence of carbon, and minimized volume fluctuations during charge and discharge processes, ensuring stable cycling. As a result, this underscores the significant potential of Mn_2O_3@CNFs [92].

2.4.1.5. Magnesium manganese oxide ($MgMn_2O_4$). In 2022, Harudin et al. [99] undertook a research study to synthesize $MgMn_2O_4$ as a cathode material tailored for Mg-ion batteries. They utilized self-propagating combustion and electrospinning techniques in this process. Due to the small size of the nanoparticles and their ability to facilitate ion intercalation and deintercalation during the charge and discharge processes, the resulting composite demonstrates excellent structural stability even after multiple cycles, consequently prolonging its cycling lifespan. Furthermore, incorporating electrospinning features enhances several aspects, including performance in capacity rate, discharge capacity, kinetic ion and electron diffusion, and electrical conductivity. They constructed a battery configuration using Mg metal as the anode, $MgMn_2O_4$ as the cathode, and $Mg(CF_3SO_3)_2$ + EC + DME as the electrolyte. Notably, compared the cathode without electrospinning, this configuration exhibits a discharge capacity that is five times higher. As depicted in Fig. 6E, the electrospun $MgMn_2O_4$ cathode demonstrates impressive charge and discharge capacities of 396 and 295 mAh g^{-1}, respectively. These results indicate the outstanding ability of the cathode, post-electrospinning, to store and release electrical energy efficiently [99].

2.4.2. Vanadium oxides

Vanadium oxide materials exhibit flexibility in chemical composition, structure, and morphology. They provide significant promise due to their impressive attributes, such as high theoretical specific capacity, elevated operating voltage, and remarkable energy density [100–104], rendering them highly suitable for energy storage applications. Nonetheless, they encounter challenges, such as low kinetic conductivity and substantial fluctuations in intercalation and de-intercalation [100,105–108]. It is suggested to use a carbon structure in conjunction with vanadium-based materials to enhance the kinetics of ion transport and mitigate volume changes [107].

Here, we provide an overview of several studies between 2019 and 2022 in which researchers have achieved significant progress in developing advanced cathode materials for Zn-ion batteries using electrospinning and heat treatment techniques.

2.4.2.1. Vanadium (V) oxide (V_2O_5). Wang et al. [109] synthesized a core-shell hierarchical hybrid fiber encapsulating V_2O_5 nanoparticles using electrospinning and calcination. This approach aimed to create a binder-free cathode for Zn-ion batteries, schematically illustrated in Fig. 7A(a). The unique core-shell hierarchical structure consists of a hollow central shell with a one-dimensional (1D) structure and an interior carbon network. This design facilitates efficient ion and electron transfer while minimizing ion diffusion paths. The researchers assembled the battery with a Zn nanosheet/CNT anode, the hybrid fiber cathode, and the polymer electrolyte. This hybrid fiber configuration markedly improved battery performance and kinetics, resulting in a capacity of 409 mAh g^{-1} at a current density of 8000 mA g^{-1}, and maintaining a columbic efficiency of 100 % after 2000 cycles. Also, by using the XRD pattern, structural changes can be observed as favorable reversible results for the insertion/extraction of Zn^{2+} ions in charge/discharge processes, indicating good cycling performance.

Additionally, Chen et al. [110] successfully synthesized V_2O_5 porous nanofibers (Fig. 7B(a)) via electrospinning and calcination techniques for use in Zn-ion batteries. With the use of ex situ XRD results, it is observed that they show reversible structural evolution and high stability of these cathodes. Additionally, BET measured the specific surface area at approximately 27.08 m^2 g^{-1}, and BJH revealed a pore size distribution of about 4 nm (Fig. 7B(b)). Therefore, these findings collectively demonstrate a mesoporous, stable structure that facilitates electrolyte diffusion and the insertion of Zn^{2+} ions. They configured the battery with Zn foil as the anode, V_2O_5 nanofibers as the cathode, and Zn $(CF_3SO_3)_2$ as the electrolyte. According to the Fig. 7B(c), this V_2O_5 porous nanofiber exhibited a reversible capacity of 319 mAh g^{-1} at a current density of 20 mA g^{-1}, retaining 81 % of their initial capacity

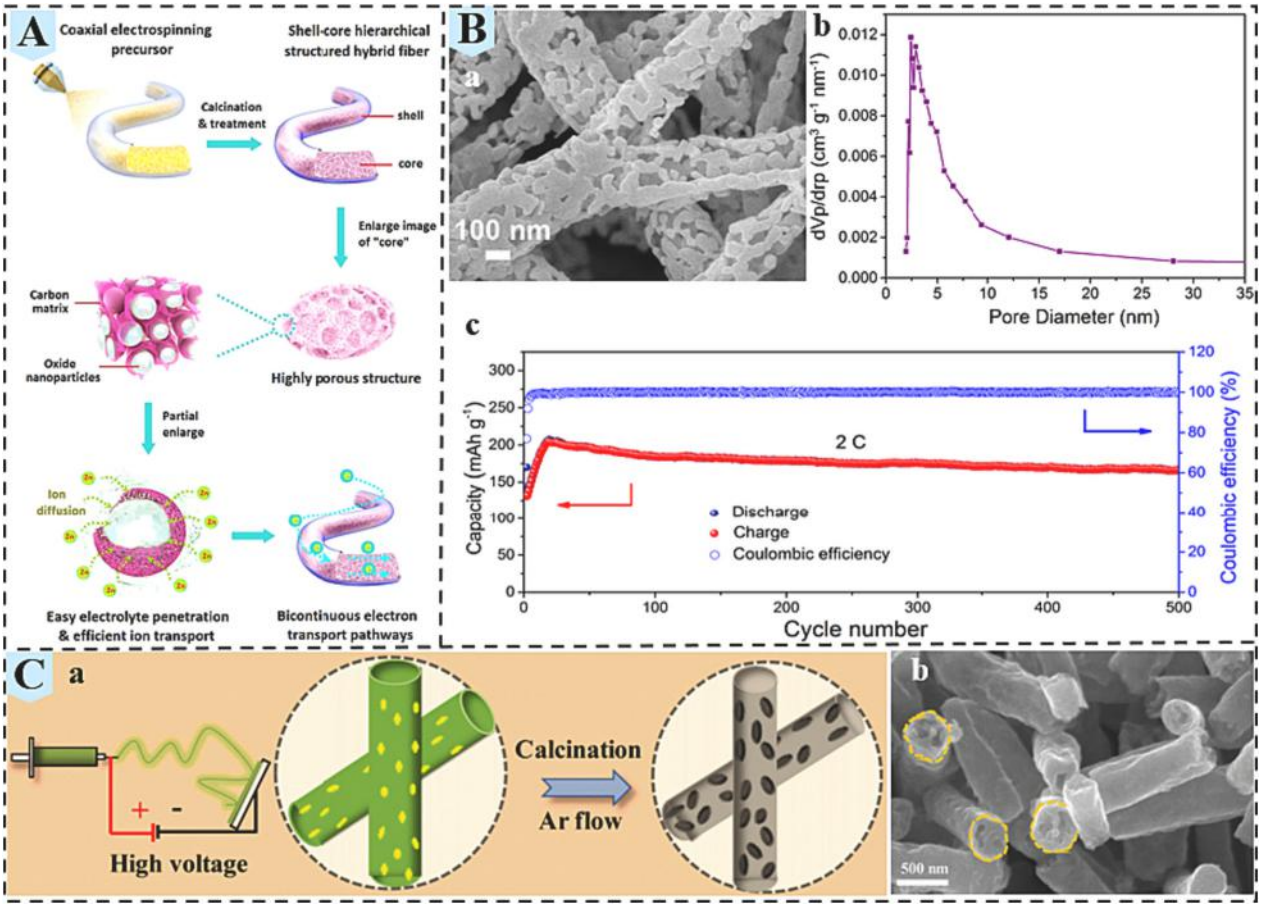

Fig. 7. A. Illustration of the Core-Shell hierarchical structured hybrid fibers; a) Schematic illustration of the synthesis process of the Core-Shell Hierarchical Structured Hybrid Fibers; b) TEM image of the hybrid fibers with V_2O_5; c) SEM images of the hybrid fibers with V_2O_5; Adapted with permission. [109] Copyright 2019, American Chemical Society. B. Illustration of the V_2O_5 nanofibers; a) SEM image of as-prepared V_2O_5 nanofibers; b) BJH plots of the pore size distribution of V_2O_5 nanofibers; Adapted with permission. [110] Copyright 2019, Elsevier. C. Illustration of the hierarchical porous VCN fibers; a) fibers preparation process; b) SEM image of VCN fibers; Adapted with permission. [111] Copyright 2020, Elsevier.

after 500 cycles, making them a promising choice for cathode materials.

Chen et al. [111] synthesized vanadium oxide nanofibers known as VCN. These nanofibers exhibited physical and chemical defects, along with a 3D porous structure, using the electrospinning and pyrolysis techniques, as presented in Fig. 7C(a). This fabrication method resulted in a hierarchical framework (Fig. 7C(b)) and a stable structure during the charge/discharge process. The physical defects, such as tiny tunnels, underground hollows, micropores, or cracks, can reduce the ion diffusion pathway, improve electrolyte accessibility, accelerate reaction kinetics, and increase electrical conductivity.

As well as, the intertwined fibrous arrangement prevents the self-clumping of active vanadium oxides, maintaining their structural integrity and ultimately improving the specific capacity of the VCN cathode. For the battery assembly, zinc foil served as the anode, VCN as the cathode, and $ZnSO_4$ as the electrolyte. The VCN cathode exhibited a specific capacity of 177 mAh g^{-1} at a current density of 1000 mA g^{-1} and maintained 111 mAh g^{-1} after 100 cycles. Additionally, it demonstrated a specific capacity of 256 mAh g^{-1} at 1000 mA g^{-1} and retained 83 % of its capacity after 1000 cycles at 5000 mA g^{-1}, showcasing the high electrochemical performance of the VCN cathode for practical applications.

Yoo et al. [112] investigated Fe-doped V_2O_5 nanorods as cathode materials for Zn-ion batteries. As depicted in Fig. 8A(a, b), these nanorods were fabricated using electrospinning and annealing techniques to adopt a nanorod structure. The battery was assembled with zinc metal as the anode, a V_2O_5-based cathode, and $Zn(CF_3SO_3)_2$ as the electrolyte. These cathodes exhibited specific capacities of 422 mAh g^{-1} at a current density of 500 mA g^{-1}, and 256 mAh g^{-1} at 2000 mA g^{-1} while retaining 85 % of cycling stability after 160 cycles at a current density of 1300 mA g^{-1}. This performance highlights their improved electrical conductivity, interaction with the electrolyte, and reduced ion diffusion path. As is evident from the results of analyses such as XRD and XPS, the outstanding improvements can be attributed to both Fe doping and the electrospun structure. This makes Fe-doped V_2O_5 nanorods a promising candidate for the next generation of energy storage devices.

In another study conducted by Yoo et al. [113], V_2O_5 nanochips with interface defects were developed by incorporating combusted graphene through electrospinning and annealing (Fig. 8B(a, b)). The resulting cathode exhibited enhanced electrochemical kinetics, reduced ion diffusion distance, improved electrical conductivity, and excellent cyclability. The battery with Zn metal as the anode, a V_2O_5-based cathode, and $Zn(CF_3SO_3)_2$ electrolyte demonstrated an impressive 74.6 % specific capacity retention after 300 cycles, achieving a value of 293.5 mAh g^{-1} at a current density of 1300 mA g^{-1}.

In another investigation, Xu et al. [114] synthesized V_2O_5@CFC, a binder-free V_2O_5 carbon fiber cloth, using electrospinning and high-temperature calcination. According to the BET results, V_2O_5@CFC exhibits a mesoporous structure (Fig. 8C(a)) with a specific surface area of 143.6 m^2 g^{-1}. This characteristic is beneficial for enhancing charge migration and solution wetting. They assembled the battery with pure Zn foil as the anode, V_2O_5@CFC as the cathode, and $ZnSO_4 + MnSO_4$ as the electrolyte. Based on Fig. 8C(b), this configuration showed a specific capacity of 132 mAh g^{-1} at a current density of 1000 mA g^{-1} and exhibited good cyclability with a capacity of 154 mAh g^{-1} at 500 mA g^{-1}

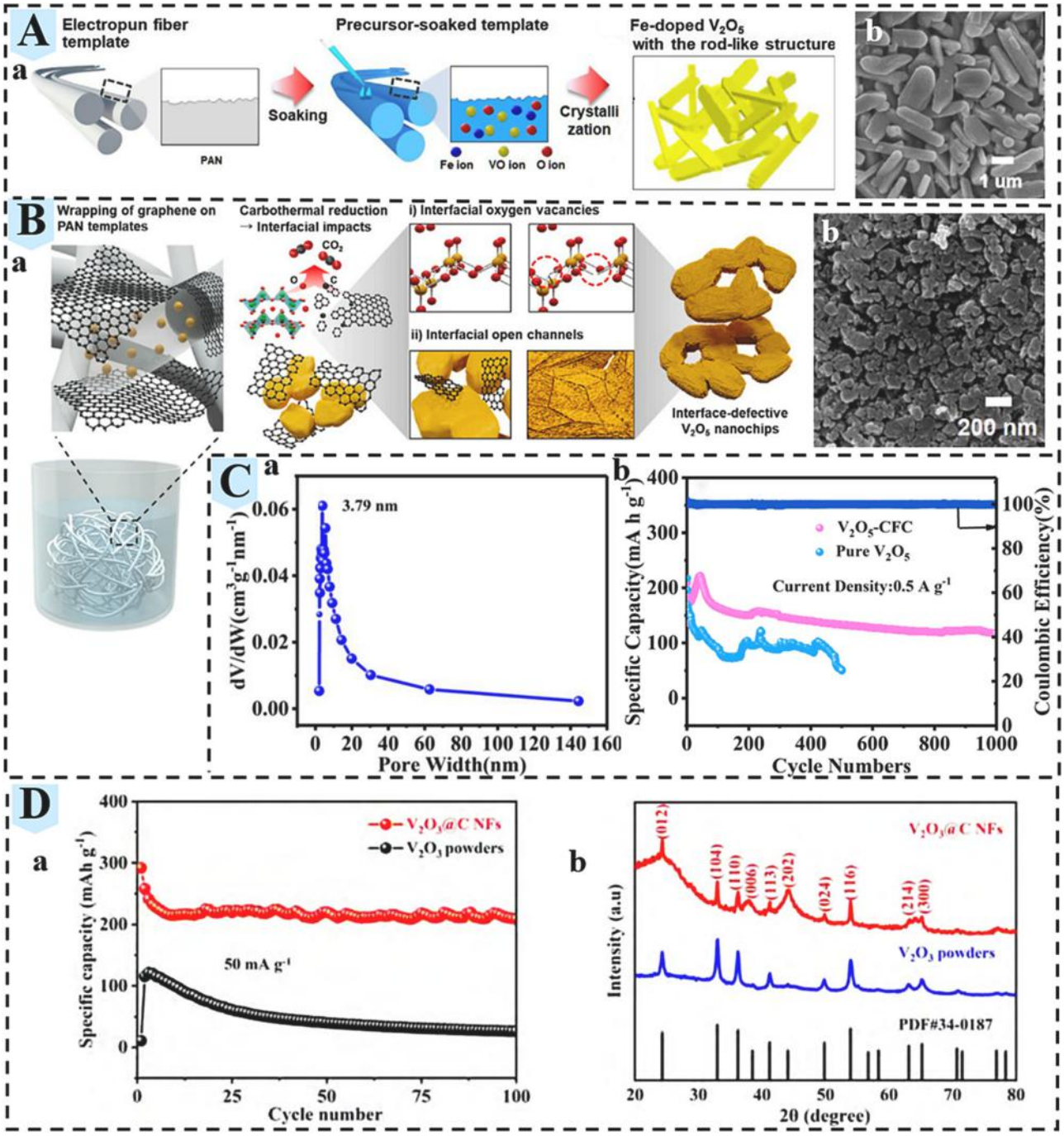

Fig. 8. A. Illustration of the Fe-doped V_2O_5 nanorods; a) Schematic illustration of the specific growth of rod-shaped Fe-doped V_2O_5; b) SEM images of bare V_2O_5; Adapted with permission 2021. [112] Copyright, Elsevier. B. Illustration of the V_2O_5 nanochips with interface defects; a) Mechanism of formation of interface-defective V_2O_5 nanochips (1G-V_2O_5-x); b) FESEM images of 1G-V_2O_5-x; Adapted with permission 2021. [113]Copyright, Elsevier. C. Illustration of the V_2O_5@CFC; a) BJH pore size distribution plots of the V_2O_5@CFC; b) Cycling performance at a current density of 500 mA g^{-1}; Adapted with permission 2022. [114] Copyright, Elsevier. D. Illustration of the V_2O_3@CNFs; a) Cycling performance of V_2O_3@CNFs and V_2O_3 electrodes; b) XRD patterns of V_2O_3@CNFs and V_2O_3; Adapted with permission. [116] Copyright 2022, American Chemical Society.

after 1000 cycles. The 3D carbon nanofiber structure displayed excellent flexibility, high electrical conductivity (alongside the carbon structure, nitrogen doping plays a crucial role in achieving high conductivity), minimal volume fluctuation (owing to the mesoporous structure and the presence of carbon), and improved kinetic reaction.

One notable study, performed by Volkov et al. [115], successfully synthesized vanadium pentoxide nanofibers, through sol-gel electrospinning and subsequent heat treatment in an air atmosphere. Incorporating nanostructured active materials into the electrodes increased battery capacity and stability. Furthermore, the increased availability of specific surface area particles in V_2O_5 led to a corresponding boost in specific capacity. The battery, composed of a Zn foil anode, electrospun nanofiber V_2O_5 cathode, and $ZnSO_4$ electrolyte, demonstrated an impressive specific capacity of 357 mAh g^{-1} at 50 mA g^{-1}. It maintained remarkable electrochemical performance even after 500 cycles, reaching more than the initial value by about 101 %. However, this capacity only amounted to 36 % of the maximum value. This discrepancy could be attributed to the presence of trapped Zn^{2+} ions, leading to a reduction

in material accessibility.

To summarize, using V_2O_5-based electrospun fibers marks a pivotal leap in the advancement of cathode materials for Zn-ion batteries, with transformative potential in energy storage and diverse applications. These materials, renowned for their unique crystalline structure and substantial theoretical specific capacity, herald a new era of enhanced battery performance and cost-effectiveness. However, the quest for optimal electrical conductivity and kinetic response continues to beckon innovation and determination [110,112–115].

2.4.2.2. Vanadium (III) oxide (V_2O_3). As mentioned above, the substantial theoretical potential of Vanadium-based oxides, combined with their extensive crystalline structure, makes them highly appealing and promising for battery applications. Among these oxides, V_2O_3 stands out with its 3D tunnel structure, which is suitable for the intercalation and deintercalation of ions. Moreover, V_2O_3 exhibits lower electrical resistance than other transition metal oxides, offering distinct advantages for efficient ion transmission. However, the fragile nature of V_2O_3 poses challenges in battery cycling due to significant volume fluctuations and

Table 1
Analysis of material & process parameters on electrospun fibers.

Materials	Electrospinning solution (Precursor/Polymer/ Molecule weight(g/mol)/ Solvent)	Electrospinning parameters (Feeding rate (ml/h)/Applied voltage (kV)/ Distance between the syringe and collector (cm)/Gauge number)	Post treatment (Temperature (°C)/ Time (h)/Atmosphere)	Fiber characterization method	Fiber structure	Ref.
MoS_2@CNFs	$(NH_4)_2MoS_4$/PAN/150000/ DMF	1/19/18/21	I: 230/2/air II: 450/2/7 % H_2-93% Ar III: 850/1/Ar	XPS/XRD/SEM/TEM/ EDX/ICP-OES	3D porous	[57]
CoS_2@CNFs	$C_4H_6CoO_4{\cdot}4H_2O$/PAN/ –/DMF	–/–/–/–	I: Peroxidized II: 900/air III: Hydrothermal synthesis 155/12 IV: 450/4/inert	XRD/XPS/SEM/TEM/ EDX/BET/BJH/TGA/ Raman	3D network	[60]
NiS_2/SC@SCNF	Ni,C/PAN/150000/DMF	1.2/19/15/21	I: 280/2/N_2 II: 800/1/N_2 III: 350/2/N_2	XRD/XPS/SEM/TEM/ EDX/TGA/Raman	3D network	[65]
$Se_{2.9}S_{5.1}$@MCNF	–/PAN,PS/150,000,192,000/ –/DMF	0.1/18/–/–	I: 250/1/air II: 900/2/N_2 III: 600/3	XRD/XPS/SEM/TEM/ BET/TGA/Raman	Multichannel	[67]
$MoSe_2$@NCNF	–/PAN/150000/DMF	–/14/–/–	I: 230/3/air II: 850/6/N_2 III: Hydrothermal synthesis 200/10 IV: 500/2/Ar	XRD/XPS/SEM/TEM/ EDX/TGA	Hierarchical core-shell	[81]
$Cu_{1.8}Se$@CNF	$Cu(CH_3COO)_2{\cdot}H_2O$/PAN/ –/DMF	2/20/–/–	I: 1000/N_2	XRD/XPS/SEM/TEM/ EDS/BET	3D	[88]
VN/N-CNF	VCl_3,H_2BDC/PAN/150000/ DMF	–/18/15/21	I: 100/4/air II: 200/4/air III: 800/2/N_2	XRD/XPS/SEM/TEM/ EDS/BET/BJH/EPR/ TGA	3D hierarchical	[71]
Mn_3O_4@HCFs	Mn_3O_4/PAN/150000/DMF	0.15/13/20/–	I: 225/7/air II: 450/3/Ar	XRD/XPS/SEM/TEM/ EDS/BET/BJH/TGA	Core-Shell	[89]
MnO_x-CNFs	Mn-MOF/PAN/130000/DMF	0.8/15/15/–	I: 280/2 h/air II: 800/2/N_2 III: 350/1.5/air	XRD/XPS/SEM/TEM/ BET/XAS	Core-shell	[91]
MnO@N-C	$Mn(Ac)_2{\cdot}4H_2O$/PVP/ 1300000/Ethanol	6/10/15/–	I: 280/1/air II: 500/2/Ar	XRD/XPS/SEM/TEM/ EDS/TG-DSC	3D porous network	[90]
V_2O_5 nanofiber	–/PVP/1300000/H_2O_2	0.5/15–18/–	I: 500/1/air	XRD/XPS/EDX/SEM/ OM	Porous and layered	[115]
VCN	$VO(acac)_2$/PAN/16000/DMF	0.6/20/18/	I: 250/1/air II: 500/2/Ar	XRD/XPS/SEM/TEM/ EDS/TGA/Raman	Hierarchical porous	[111]
Mn_2O_3	$Mn(Ac)_2{\cdot}4H_2O$/PVP/ 1300000/Ethanol	6/25/15/–	I: 500/2/air	XRD/SEM/TEM/TG-DSC	3D nano-porous	[92]
V_2O_5 nanofiber	NH_4VO_3- $H_2C_2O_4{\cdot}2H_2O$/PVP/ 1300000/DMF	0.6/16/15/21	I: 400/2	XRD/XPS/SEM/TEM/ BET/BJH/Raman	Porous nanofiber	[110]
Fe-doped V_2O_5 nanorods	$VOSO_4{\cdot}xH_2O$,$FeCl_3.6H_2O$/ PAN/150000/DMF	400/10/10/–	I: 600/8/air	XRD/XPS/SEM/TEM/ EDS/UV–vis	Nanorod	[112]
V_2O_5 nanochips	–/PAN/150000/DMF/	400/10/10/–	I: 400/8/air	XRD/XPS/SEM/TEM/ Raman/UV–vis	Nanochips	[113]
VOC-NF	$C_{10}H_{14}O_5V$/PAN/–/DMF	1.2/16/15/23	I: 800/3/H2-Ar (10 %) II: 200/24/steam atmosphere III: Hydrothermal synthesis	XRD/XPS/SEM/TEM/ EDX/TGA/Raman	Nanodots encapsulated in CNFs	[117]
V_2O_5@CFC	V_2O_5 nanosheets/PAN/ 150000/DMF	0.1/17/15/23	I: 700/2/Ar	XRD/XPS/SEM/TEM/ BET/BJH/EDX/TGA/ Raman	3D network	[114]
V_2O_3@CNFs	$C_{15}H_{21}O_6V$/PAN/1500000/ DMF	1/15/16/–	I: 235/air II: 700/Ar	XRD/XPS/SEM/TEM/ EDS/TGA/Raman	Tunnel-like 3D	[116]
V_2O_5 nanoparticles	V_2O_5 nanoparticles/PAN, PMMA/–/DMF	–/10–12/9/17–23	I: 280/1/air II: 700/N2 III: 400/air	XRD/XPS/SEM/TEM/ BET/BJH/EDS/TGA/ Raman	Core-shell hierarchical	[109]
$MgMn_2O_4$	$MgMn_2O_4$/PAN/–/DMF	1/18/15/–	I: 300/2	XRD/SEM/OM/EDS	Nanofiber	[99]

sluggish charge transfer kinetics. In 2022, Liu et al. [116] addressed these issues by creating a binder-free V_2O_3@CNFs, a flexible cathode material for zinc-ion batteries, through the utilization of electrospinning, subsequently followed by stabilization and carbonization processes. The battery configuration included Zn foil coated with carbon (Zn@CC) as the anode, V_2O_3@CNFs as the cathode, and $Zn(CF_3SO_3)_2$ as the electrolyte. As shown in Fig. 8D(a), this battery demonstrated an initial capacity of 220 mAh g^{-1} at 50 mA g^{-1}. After 1000 cycles, it exhibited a capacity of 120/65 mAh g^{-1} at 200/2000 mA g^{-1}, indicating good cycling stability. Incorporating carbon into V_2O_3@CNFs significantly enhanced the electrical conductivity of the composite, leading to improved charge transfer kinetics. Additionally, the electrospinning process contributed to enhanced structural integrity, facilitating faster ion transfer kinetics and creating more active reaction sites, as evidenced by the XRD pattern (Fig. 8D(b)). These improvements resulted in the battery showcasing excellent electrochemical performance and cycling stability [116].

2.4.2.3. Vanadium (II) oxide (VO). In 2022, Liu et al. [117] successfully synthesized VO nanodots by incorporating them into carbon nanowires, forming VOC-NF through electrospinning and calcination techniques. This novel binder-free cathode was designed for use in Zn-ion batteries. The distinctive nanostructure of VOC-NF plays a crucial role in enhancing battery performance. Reducing the distance for ion transfer facilitates efficient ion diffusion and electron transfer processes. Furthermore, VOC-NF exhibits excellent electrical conductivity and stable structure, further contributing to its effectiveness as a cathode material. In the battery assembly, a metallic zinc foil is the anode, VOC-NF is the cathode, and $Zn(CF_3SO_3)_2$ is the electrolyte. The battery showcased impressive performance characteristics, with a specific capacity of 319 mAh g^{-1} at 100 mA g^{-1} and 215 mAh g^{-1} at 20000 mA g^{-1}. Remarkably, even after 18,000 cycles, it retained 63 % of its original capacity, demonstrating exceptional cycle stability. Given the remarkable performance exhibited by this cathode material, it holds great promise for application in future battery technologies [117].

All the relevant details regarding electrospinning technique parameters and methods for characterizing produced fiber and fiber structure have been organized in Table 1. Additionally, the performance of various electrospun cathode materials for multivalent batteries, such as metal sulfides, metal nitrides, metal selenides, and metal oxides, is summarized in Table 2. These tables facilitate a comprehensive comparison of research findings. Researchers can rely on these tables as valuable resources for obtaining the required information.

3. Advantages and challenges of electrospun cathodes

As previously mentioned, multivalent batteries can address the limitations of Li-ion batteries and offer higher energy density. However, their progress faces challenges due to specific cathode materials. These materials encounter energy density and diffusion kinetics difficulties because of their higher electrostatic interaction with multivalent ions compared to monovalent ions [17,118]. The selection of suitable cathode materials is also restricted by the challenge of enabling reversible multivalent ion intercalation. This challenge involves overcoming sluggish ion diffusion within the host matrix structure due to interactions with other species present in the electrolyte. Therefore, one of the primary challenges in advancing multivalent battery technology lies in identifying cathode materials capable of reversibly storing and releasing these multivalent cations [120].

On another note, electrospinning is one of the most promising and widely embraced methods for producing nanofibers with adjustable morphologies, offering various advantages [40,121–124]. One significant advantage of the electrospinning technique is its ability to create cathodes without using binders. This not only prevents unwanted reactions between the electrolyte and binders in these electrodes but also improves their overall performance and durability [125]. Additionally, not having binders allows for a more effective use of the active material in the cathode and strengthens the connection between the active material and the current collector [126]. Electrodes fashioned from these nanofibers exhibit exceptional characteristics: they boast a substantial surface area that this increased surface area and enhanced porosity, provides additional sites for electrochemical reactions, thereby boosting cathode performance and so leading to overall improvements in capacity and battery performance [122,127]. Electrospun cathodes also play a pivotal role in enhancing cyclability by reducing electrode fluctuations during charge and discharge cycles, ultimately extending the

Table 2
Comparison between electrospun nanofibers cathodes for multivalent batteries.

Battery	Cathode	Binder in cathode (Yes/No)	Anode	Electrolyte	Results: Initial capacity (mAh g^{-1})	Current density (mA g^{-1})	Cycle count	Capacity (mAh g^{-1})	Capacity retention (%)	Ref.
Al-ion	MoS_2@CNFs	N	Al foil	[EMIm]Cl + $AlCl_3$	293.2	100	200	126.6	43.17	[57]
	CoS_2@CNFs	N			–	200	500	80	–	[60]
	NiS_2/SC@SCNF	Y			–	500	500	76	–	[65]
	$Se_{2.9}S_{5.1}$@MCNF	N			–	500	3000	187	–	[67]
	$MoSe_2$@NCNF	Y			296.3	100	200	169.9	57.34	[81]
	$Cu_{1.8}Se$@CNF	Y			410	2000	5000	152.12	37.10	[88]
Zn-ion	VN/N-CNF	N	Zinc plate	$Zn(CF_3SO_3)_2$	–	50,000	30,000	482	–	[71]
	Mn_3O_4@HCFs	Y	Zn foil	$ZnSO_4 + MnSO_4$	100	400	1300	225	225	[89]
	MnO_x-CNFs	N			–	1000	100	220	71	[91]
	MnO@N-C	Y		$ZnSO_4$	~20	500	200	176.3	–	[90]
	V_2O_5 nanofiber	Y			–	50	500	357	–	[115]
	VCN	Y			177	1000	100	111	62.71	[111]
	Mn_2O_3	Y		Hydrogel	–	2000	1000	104	–	[92]
	V_2O_5 nanofiber	Y		$Zn(CF_3SO_3)_2$	393.82	20	500	319	81	[110]
	Fe-doped V_2O_5 nanorods	Y			–	80	500	422	–	[112]
	V_2O_5 nanochips	Y			393.46	1300	300	293.5	74.6	[113]
	VO-CNF	N			319	100	5000	207.35	65	[117]
	V_2O_5@CFC	N		$ZnSO_4 + MnSO_4$	–	500	1000	154	–	[114]
	V_2O_3@CNFs	N	Zn@CC	$Zn(CF_3SO_3)_2$	~240	2000	1000	~75	31.2	[116]
	V_2O_5 nanoparticles	N	Zn nanosheet	Polymeric	409	8000	2000	390.59	95.8	[109]
Mg-ion	$MgMn_2O_4$	Y	Mg metal	$Mg(CF_3SO_3)_2$ + EC + DME	295	–	–	–	–	[99]

lifespan of the electrodes [123,128]. Moreover, they enable faster charge and discharge kinetics thanks to their substantial surface area and shortened diffusion paths for ions and electrons [122,129]. Electrospinning is noteworthy for its scalability and flexibility. Its scalability enables cost-effective mass production, while its flexibility allows for using various materials, such as ceramics, polymers, and composites [130–132]. Another aspect of this flexibility involves making modifications, like N_2 doping and integrated carbon nanofibers as a conductive matrix, which can enhance specific properties like electrical conductivity [133]. Furthermore, electrospinning allows for the creating of unique cathode structures, including core-shell formations, nanotubular designs, and hierarchical architectures, all of which enhance electrochemical performance and durability [40,134]. These advantages make position them a promising choice for advancing energy storage and conversion technologies.

Despite the mentioned advantages, the electrospinning method for cathode production presents various challenges. One of these challenges lies in the variability of morphologies resulting from parameter adjustments. While this variability can be advantageous in certain situations, it can pose difficulties when striving for consistent morphologies over time [135]. Moreover, the electrospinning process involves a solvent-rich solution, leading to uncontrollable structural pores in the nanofibers during solvent evaporation, making morphology control and reproducibility challenging [136]. Additionally, preparing electrospinning solutions often necessitates using organic and toxic solvents, which can have adverse environmental impacts [136]. Polyacrylonitrile typically serves as the base polymer in electrospinning techniques. However, its suitability for specific purposes, such as hydrophilic or hydrophobic environment, must be carefully considered. For instance, it may need to be combined with other materials or make adjustments to the calcination duration [138]. Another challenge lies in striking a balance between achieving high energy density and maintaining the flexibility of fibers. For the utilization of electrospun cathodes, achieving an optimal active material loading is crucial to ensure sufficient energy density and overall better performance. However, excessive active material loading may compromise the mechanical flexibility of the fibers [139]. Furthermore, while cathode porosity is advantageous, it must fall within a critical range to ensure effective electrolyte penetration and charge transfer [140]. A larger surface area may also reduce the columbic efficiency in the initial cycles. If the porosity exceeds a critical range, thick solid electrolyte interphase (SEI) films may develop due to extensive surface contact between the electrode and electrolytes, leading to a higher irreversible capacity [141]. As indicated earlier, most cathodes exhibit a mesoporous structure, which facilitates ion diffusion but negatively affects the flexibility and durability of CNFs [142]. Additionally, electrospinning imposes limitations on the types of materials that can be synthesized, and achieving uniform nanofibers without defects, such as beads, can be challenging [143].

4. Future directions

A review of current literature reveals that cathodes designed for various multivalent batteries, including Al-ion, Zn-ion, and Mg-ion batteries, utilize electrospinning and post-treatment techniques. In the case of Al-ion batteries, strong Coulombic ion–lattice interactions result in kinetic limitations in battery processes. Moreover, the intense electrostatic interaction between Mg ions and the host lattice results in impractically long durations for ion intercalation/deintercalation due to low Mg^{2+} diffusion rates [144]. In Zn-ion batteries, limitations arise from the strong electrostatic repulsion between Zn^{2+} ions and the cathode material lattice [145]. In the broader context of multivalent energy storage systems, identifying electrode materials capable of serving as durable hosts for accommodating a large number of ions, while ensuring rapid release kinetics, remains a significant challenge. The electrospinning technique, with its unique features, offers a promising solution to address these challenges. Researchers can employ electrospun fibers as cathodes, anodes, electrolytes, and separators to tackle issues in Al-ion, Zn-ion, and Mg-ion batteries.

Notably, as of our knowledge cutoff date, there are no reported instances of electrospun cathodes being employed for calcium-ion batteries. Calcium stands out as the fifth most abundant element in the Earth's crust, 25,000 times more abundant than lithium. Calcium is non-toxic, ensuring environmental safety [146,147]. Moreover, Ca^{2+} exhibits a low polarization profile similar to lithium, boasting a reduction potential of −2.87 V vs. SHE, which is closely similar to Li's (−3.04 V vs. SHE). Additionally, it offers an impressive volume-specific capacity of approximately 1073 mAh ml^{-1} and demonstrates enhanced kinetic diffusion. This attribute plays a pivotal role in reducing overall load density, contributing to more excellent reversibility in capacity [148,149]. However, calcium-ion batteries do face specific challenges. They primarily stem from the limited availability of suitable calcium salts for electrolytes the electrode materials. This limitation, particularly about to electrodes, arises from the significantly larger ionic radius of Ca^{2+} (100 pm) compared to Li^{+} (70 pm) [149]. This difference in ion size can lead to premature structural degradation due to substantial volume changes [150]. Due to the electrospinning technique's ability to create materials with a high surface area, porous structure, and cost-effectiveness, calcium-ion batteries hold significant promise. Crafting electrodes using this method could accelerate the development of calcium-ion battery technology and help address issues related to ion radius.

Additionally, as demonstrated in this article, and considering the exclusive use of elements such as sulfides and selenides in aluminum-ion batteries, along with the preference for nitrides and oxides in zinc and magnesium-ion batteries, it motivates researchers to explore these choices further in the field of battery technology.

5. Conclusions

The quest for high-performance materials in energy storage systems has prompted researchers to explore metal sulfides, nitrides, selenides, and oxides as promising candidates for cathode materials in multivalent batteries. Within the scope of this review, the core principles of electrospinning, a technique synergistically combined with various methodologies, were explored. These methodologies enhance the overall approach by combining annealing, pyrolysis, sulfidation, calcination, selenization, and hydrothermal reaction processes, to enhance the overall approach. The incorporation of elements such as Fe and N is also examined. This combination results in the creation of nanofibers with distinct structures, including multichannel fibers, core-shell hierarchical hybrid fibers, defect-rich fibers at the chemical and interface levels, as well as nanorods and nanochip fibers, all designed for integration into multivalent batteries as cathodes. These cathodes exhibit remarkable performance, attributed to their distinctive structures. These structures facilitate optimal contact between the active material and the electrolyte, reduce ion diffusion distances, and minimize volume fluctuations while enhancing kinetic performance. Additionally, in the case of carbon-based structures, they provide mechanical stability and high conductivity. This thorough review deepens our comprehension of recent progress and challenges regarding electrospun cathodes in multivalent batteries. It offers valuable perspectives for future researchers and enthusiasts interested in multivalent battery cathodes. This analysis aims to supply meaningful insights to individuals conducting research in this domain, ensuring a clear understanding of the strengths and limitations of these materials within the multivalent battery technology field.

CRediT authorship contribution statement

Bahar Zare: Investigation, Supervision, Writing – original draft, Writing – review & editing. **Sayed Khatiboleslam Sadrnezhaad:** Investigation, Supervision, Writing – original draft, Writing – review &

editing.

Declaration of competing interest

The authors declare that they have no known competing financial interests or personal relationships that could have appeared to influence the work reported in this paper.

Data availability

No data was used for the research described in the article.

Acknowledgements

The authors sincerely appreciate the invaluable and helpful guidance and support provided by Dr. Foad Soleimani, Ms. Fatemeh Sousani, and Mr. Hosein Mahtabpour.

References

[1] H. Wang, S. Chen, C. Fu, Y. Ding, G. Liu, Y. Cao, Z. Chen, Recent advances in conversion-type electrode materials for post lithium-ion batteries, ACS Mater Lett. 3 (2021) 956–977, https://doi.org/10.1021/acsmaterialslett.1c00043.
[2] F. Maroni, S. Dongmo, C. Gauckler, M. Marinaro, M. Wohlfahrt-Mehrens, Through the maze of multivalent-ion batteries: a critical review on the status of the research on cathode materials for Mg^{2+} and Ca^{2+} ions insertion, Batter Supercaps. 4 (2021), https://doi.org/10.1002/batt.202000330.
[3] S. Zhang, T. Long, H.-Z. Zhang, Q.-Y. Zhao, F. Zhang, X.-W. Wu, X.-X. Zeng, Electrolytes for multivalent metal-ion batteries: current status and future prospect, ChemSusChem 15 (2022), https://doi.org/10.1002/cssc.202200999.
[4] C. Wu, H. Tan, W. Huang, C. Liu, W. Wei, L. Chen, Q. Yan, The strategies to improve the layered-structure cathodes for aqueous multivalent metal-ion batteries, Mater Today Energy. 19 (2021) 100595, https://doi.org/10.1016/J.MTENER.2020.100595.
[5] P. Canepa, G. Sai Gautam, D. Hannah, R. Malik, M. Liu, K. Gallagher, K. Persson, G. Ceder, Odyssey of multivalent cathode materials: open questions and future challenges, Chem. Rev. 117 (2017), https://doi.org/10.1021/acs.chemrev.6b00614.
[6] C. Wang, Z. Pan, H. Chen, X. Pu, Z. Chen, MXene-based materials for multivalent metal-ion batteries, Batteries 9 (2023), https://doi.org/10.3390/batteries9030174.
[7] D. Monti, A. Ponrouch, R.B. Araujo, F. Barde, P. Johansson, M.R. Palacín, Multivalent batteries-prospects for high energy density: Ca batteries, Front. Chem. 7 (2019), https://doi.org/10.3389/fchem.2019.00079.
[8] A. Ponrouch, J. Bitenc, R. Dominko, N. Lindahl, P. Johansson, M.R. Palacin, Multivalent rechargeable batteries, Energy Storage Mater. 20 (2019) 253–262, https://doi.org/10.1016/J.ENSM.2019.04.012.
[9] Y. Chen, K. Fan, Y. Gao, C. Wang, Challenges and perspectives of organic multivalent metal-ion batteries, Adv. Mater. 34 (2022), https://doi.org/10.1002/adma.202200662.
[10] R.K. Guduru, J.C. Icaza, A brief review on multivalent intercalation batteries with aqueous electrolytes, Nanomaterials 6 (2016), https://doi.org/10.3390/nano6030041.
[11] Y. Liang, H. Dong, D. Aurbach, Y. Yao, Current status and future directions of multivalent metal-ion batteries, Nat. Energy 5 (2020), https://doi.org/10.1038/s41560-020-0655-0.
[12] Y.E. Durmus, H. Zhang, F. Baakes, G. Desmaizieres, H. Hayun, L. Yang, M. Kolek, V. Küpers, J. Janek, D. Mandler, S. Passerini, Y. Ein-Eli, Side by side battery technologies with lithium-ion based batteries, Adv Energy Mater. 10 (2020) 2000089, https://doi.org/10.1002/aenm.202000089.
[13] J. Xie, Q. Zhang, Recent progress in multivalent metal (Mg, Zn, Ca, and Al) and metal-ion rechargeable batteries with organic materials as promising electrodes, Small 15 (2019), https://doi.org/10.1002/smll.201805061.
[14] S. Chen, D. Zhao, C. Long, G. Liu, Y. Ding, Y. Cao, Z. Chen, Emerging intercalation cathode materials for multivalent metal-ion batteries: status and challenges, Small Struct. 2 (2021), https://doi.org/10.1002/sstr.202100082.
[15] M.S. Kiai, O. Eroglu, N. Aslfattahi, Metal-ion batteries: achievements, challenges, and prospects, Crystals (Basel) 13 (2023) 1002, https://doi.org/10.3390/cryst13071002.
[16] A. Rutt, J.-X. Shen, M. Horton, J. Kim, J. Lin, K.A. Persson, Expanding the material search space for multivalent cathodes, ACS Applied Materials & Interfaces 14 (2022) 44367–44376, https://doi.org/10.1021/acsami.2c11733.
[17] E. Karapidakis, D. Vernardou, Progress on V_2O_5 cathodes for multivalent aqueous batteries, Materials 14 (2021), https://doi.org/10.3390/ma14092310.
[18] D. Kundu, S. Hosseini Vajargah, L. Wan, B. Adams, D. Prendergast, L.F. Nazar, Aqueous vs. nonaqueous Zn-ion batteries: consequences of the desolvation penalty at the interface, Energy Environ. Sci. 11 (2018) 881–892, https://doi.org/10.1039/C8EE00378E.
[19] H. Tang, C. Zuo, F. Xiong, C. Pei, S. Tan, P. Luo, W. Yang, Q. An, L. Mai, Flexible three-dimensional-networked iron vanadate nanosheet arrays/carbon cloths as high-performance cathodes for magnesium ion batteries, Sci. China Mater. 65 (2022) 2197–2206, https://doi.org/10.1007/s40843-021-2000-y.
[20] M. Liu, Z. Rong, R. Malik, P. Canepa, A. Jain, G. Ceder, K.A. Persson, Spinel compounds as multivalent battery cathodes: a systematic evaluation based on ab initio calculations, Energy Environ. Sci. 8 (2015) 964–974, https://doi.org/10.1039/C4EE03389B.
[21] W. Liu, T. Placke, K.T. Chau, Overview of batteries and battery management for electric vehicles, Energy Rep. 8 (2022) 4058–4084, https://doi.org/10.1016/j.egyr.2022.03.016.
[22] H. Tang, Z. Peng, L. Wu, F. Xiong, C. Pei, Q. An, L. Mai, Vanadium-based cathode materials for rechargeable multivalent batteries: challenges and opportunities, Electrochemical Energy Reviews 1 (2018) 169–199, https://doi.org/10.1007/s41918-018-0007-y.
[23] Q. Tang, Q. Ke, Q. Chen, X. Zhang, J. Su, C. Ning, L. Fang, Flexible, breathable, and self-powered patch assembled of electrospun polymer triboelectric layers and polypyrrole-coated electrode for infected chronic wound healing, ACS Appl. Mater. Interfaces 15 (2023) 17641–17652, https://doi.org/10.1021/acsami.3c00500.
[24] B.F. Adamu, J. Gao, E.K. Gebeyehu, K.A. Beyene, M.G. Tadesse, E.Z. Liyew, Self-responsive electrospun nanofibers wound dressings: the future of wound care, Adv. Mater. Sci. Eng. 2022 (2022) 2025170, https://doi.org/10.1155/2022/2025170.
[25] Y. Li, J. Wang, Y. Wang, W. Cui, Advanced electrospun hydrogel fibers for wound healing, Compos B Eng. 223 (2021) 109101, https://doi.org/10.1016/J.COMPOSITESB.2021.109101.
[26] M. Reise, S. Kranz, A. Guellmar, R. Wyrwa, T. Rosenbaum, J. Weisser, A. Jurke, M. Schnabelrauch, M. Heyder, D.C. Watts, B.W. Sigusch, Coaxial electrospun nanofibers as drug delivery system for local treatment of periodontitis, Dent. Mater. 39 (2023) 132–139, https://doi.org/10.1016/J.DENTAL.2022.12.008.
[27] S.M. Costa, R. Fangueiro, D.P. Ferreira, Drug delivery systems for photodynamic therapy: the potentiality and versatility of electrospun nanofibers, Macromol Biosci. 22 (5) (2022) e2100512, https://doi.org/10.1002/mabi.202100512.
[28] Z. Krysiak, U. Stachewicz, Electrospun fibers as carriers for topical drug delivery and release in skin bandages and patches for atopic dermatitis treatment, Wiley Interdiscip. Rev. Nanomed. Nanobiotechnol. 15 (2022), https://doi.org/10.1002/wnan.1829.
[29] P.J. Espinoza-Montero, M. Montero-Jiménez, S. Rojas-Quishpe, C.D. Alcívar León, J. Heredia-Moya, A. Rosero-Chanalata, C. Orbea-Hinojosa, J.L. Piñeiros, Nude and modified electrospun nanofibers, application to air purification, Nanomaterials 13 (2023), https://doi.org/10.3390/nano13030593.
[30] Y. Deng, T. Lu, X. Zhang, Z. Zeng, R. Tao, Q. Qu, Y. Zhang, M. Zhu, R. Xiong, C. Huang, Multi-hierarchical nanofiber membrane with typical curved-ribbon structure fabricated by green electrospinning for efficient, breathable and sustainable air filtration, J Memb Sci. 660 (2022) 120857, https://doi.org/10.1016/J.MEMSCI.2022.120857.
[31] H. Wu, R. Xie, Y. Hao, J. Pang, H. Gao, F. Qu, M. Tian, C. Guo, B. Mao, F. Chai, Portable smartphone-integrated AuAg nanoclusters electrospun membranes for multivariate fluorescent sensing of Hg^{2+}, Cu^{2+} and l-histidine in water and food samples, Food Chem. 418 (2023) 135961, https://doi.org/10.1016/J.FOODCHEM.2023.135961.
[32] A. Abutaleb, CuNi alloy NPs anchored on electrospun PVDF-HFP NFs catalyst for H2 production from sodium borohydride, Polymers (Basel) 15 (2023), https://doi.org/10.3390/polym15030474.
[33] A. Abutaleb, I.M. Maafa, N. Zouli, A. Yousef, M.M. El-Halwany, Electrospun co nanoparticles@PVDF-HFP nanofibers as efficient catalyst for dehydrogenation of sodium borohydride, Polymers (Basel) 15 (2023), https://doi.org/10.3390/polym15030597.
[34] S. Zhu, L. Nie, Progress in fabrication of one-dimensional catalytic materials by electrospinning technology, Journal of Industrial and Engineering Chemistry 93 (2021) 28–56, https://doi.org/10.1016/J.JIEC.2020.09.016.
[35] A.I. Abdel-Salam, S.Y. Attia, S.G. Mohamed, F.I. El-Hosiny, M.A. Sadek, M. M. Rashad, Designing a hierarchical structure of nickel-cobalt-sulfide decorated on electrospun N-doped carbon nanofiber as an efficient electrode material for hybrid supercapacitors, Int. J. Hydrogen Energy 48 (2023) 5463–5477, https://doi.org/10.1016/J.IJHYDENE.2022.11.134.
[36] P. Fan, C. Ye, L. Xu, One-dimensional nanostructured electrode materials based on electrospinning technology for supercapacitors, Diamond Relat. Mater. 134 (2023) 109803, https://doi.org/10.1016/J.DIAMOND.2023.109803.
[37] C. Kuchi, A.L. Narayana, O.M. Hussain, P.S. Reddy, Electrospun TiO_2 nanofiber electrodes for high performance supercapacitors, Mater Res Express. 7 (2020), https://doi.org/10.1088/2053-1591/ab688c.
[38] Y. Liu, B. Luo, H. Liu, M. He, R. Wang, L. Wang, Z. Quan, J. Yu, X. Qin, 3D printed electrospun nanofiber-based pyramid-shaped solar vapor generator with hierarchical porous structure for efficient desalination, Chem. Eng. J. 452 (2023) 139402, https://doi.org/10.1016/J.CEJ.2022.139402.
[39] L. Niu, X. Li, Y. Zhang, H. Yang, J. Feng, Z. Liu, Electrospun lignin-based phase-change nanofiber films for solar energy storage, ACS Sustainable Chemistry & Engineering 10 (2022) 13081–13090, https://doi.org/10.1021/acssuschemeng.2c03462.
[40] S.H. Senthilkumar, B. Ramasubramanian, R.P. Rao, V. Chellappan, S. Ramakrishna, Advances in electrospun materials and methods for Li-ion batteries, Polymers (Basel) 15 (2023), https://doi.org/10.3390/polym15071622.
[41] M. Qian, W. Zhang, G. Luo, C. Wu, W. Qin, Air-stabilized pore structure engineering of antimony-based anode by electrospinning for potassium ion batteries, J. Colloid Interface Sci. 633 (2023) 352–361, https://doi.org/10.1016/J.JCIS.2022.11.121.

[42] J. Wang, Z. Wang, J. Ni, L. Li, Electrospinning for flexible sodium-ion batteries, Energy Storage Mater. 45 (2022) 704–719, https://doi.org/10.1016/J.ENSM.2021.12.022.
[43] Y.-H. Nien, S.-W. Zhuang, J.-C. Chou, P.-H. Yang, C.-H. Lai, P.-Y. Kuo, C.-S. Ho, Y.-T. Wu, R.-H. Syu, P.-F. Chen, Photovoltaic measurement under different illumination of the dye-sensitized solar cell with the photoanode modified by Fe_2O_3/g-C_3N_4/TiO_2 heterogeneous nanofibers prepared by electrospinning with dual jets, IEEE Trans. Semicond. Manuf. 36 (2023) 291–297, https://doi.org/10.1109/TSM.2023.3235762.
[44] L. Li, S. Peng, J.K.Y. Lee, D. Ji, M. Srinivasan, S. Ramakrishna, Electrospun hollow nanofibers for advanced secondary batteries, Nano Energy 39 (2017) 111–139, https://doi.org/10.1016/J.NANOEN.2017.06.050.
[45] S. Liu, M. Kok, Y. Kim, J.L. Barton, F.R. Brushett, J. Gostick, Evaluation of electrospun fibrous mats targeted for use as flow battery electrodes, J. Electrochem. Soc. 164 (2017) A2038–A2048, https://doi.org/10.1149/2.1301709jes.
[46] Y. Wang, Y. Liu, Y. Liu, Q. Shen, C. Chen, F. Qiu, P. Li, L. Jiao, X. Qu, Recent advances in electrospun electrode materials for sodium-ion batteries, Journal of Energy Chemistry 54 (2021) 225–241, https://doi.org/10.1016/J.JECHEM.2020.05.065.
[47] M. Wang, Y. Wu, M. Qiu, X. Li, C. Li, R. Li, J. He, G. Lin, Q. Qian, Z. Wen, X. Li, Z. Wang, Q. Chen, Q. Chen, J. Lee, Y.W. Mai, Y. Chen, Research progress in electrospinning engineering for all-solid-state electrolytes of lithium metal batteries, Journal of Energy Chemistry 61 (2021) 253–268, https://doi.org/10.1016/J.JECHEM.2021.02.023.
[48] C.W. Chang, W.C. Lai, A strategy for preparing solid polymer electrolytes via the electrospinning process, J. Taiwan Inst. Chem. Eng. 116 (2020) 279–285, https://doi.org/10.1016/J.JTICE.2020.11.012.
[49] B. Abdulkadir, J. Dennis, A. Adam, A. Al-Dhahebi, M. Shukur, Novel electrospun separator-electrolyte based on PVA-K_2CO_3 -SiO_2 -cellulose nanofiber for application in flexible energy storage devices, J. Appl. Polym. Sci. 139 (2022) 52308, https://doi.org/10.1002/app.52308.
[50] M. Toriello, M. Afsari, H.K. Shon, L.D. Tijing, Progress on the fabrication and application of electrospun nanofiber composites, Membranes (Basel) 10 (2020) 1–35, https://doi.org/10.3390/membranes10090204.
[51] A. Haider, S. Haider, I.K. Kang, A comprehensive review summarizing the effect of electrospinning parameters and potential applications of nanofibers in biomedical and biotechnology, Arab. J. Chem. 11 (2018) 1165–1188, https://doi.org/10.1016/J.ARABJC.2015.11.015.
[52] H.M. Ibrahim, A. Klingner, A review on electrospun polymeric nanofibers: production parameters and potential applications, Polym. Test. 90 (2020) 106647, https://doi.org/10.1016/J.POLYMERTESTING.2020.106647.
[53] H. Zhou, Z. Shi, X. Wan, H. Fang, D.G. Yu, X. Chen, P. Liu, The relationships between process parameters and polymeric nanofibers fabricated using a modified coaxial electrospinning, Nanomaterials 9 (2019), https://doi.org/10.3390/nano9060843.
[54] F. Soleimani, M. Mazaheri, C. Pellerin, R. Bagheri, On the importance of noncrystalline phases in semicrystalline electrospun nanofibers, ACS Appl Polym Mater. 3 (2021) 6315–6325, https://doi.org/10.1021/acsapm.1c01088.
[55] S. Kailasa, M.S.B. Reddy, M.R. Maurya, B.G. Rani, K.V. Rao, K.K. Sadasivuni, Electrospun nanofibers: materials, synthesis parameters, and their role in sensing applications, Macromol Mater Eng. 306 (2021) 2100410, https://doi.org/10.1002/mame.202100410.
[56] F. Ciucci, J. Wu, J.-K. Kim, Molybdenum disulfide based nanomaterials for rechargeable batteries, Chemistry (Easton) 26 (2020), https://doi.org/10.1002/chem.201905524.
[57] W. Yang, H. Lu, Y. Cao, B. Xu, Y. Deng, W. Cai, Flexible free-standing MoS_2/carbon nanofibers composite cathode for rechargeable aluminum-ion batteries, ACS Sustainable Chemistry & Engineering 7 (2019) 4861–4867, https://doi.org/10.1021/acssuschemeng.8b05292.
[58] Y. Liu, C. Cui, Y. Liu, W. Liu, J. Wei, Application of MoS_2 in the cathode of lithium sulfur batteries, RSC Adv. 10 (2020) 7384–7395, https://doi.org/10.1039/C9RA09769D.
[59] F. Yang, X. Feng, P.-A. Glans, J. Guo, MoS_2 for beyond lithium-ion batteries, APL Mater. 9 (2021) 050903, https://doi.org/10.1063/5.0050118.
[60] R. Zhuang, Z. Huang, S. Wang, J. Qiao, J.C. Wu, J. Yang, Binder-free cobalt sulfide@carbon nanofibers composite films as cathode for rechargeable aluminum-ion batteries, Chem. Eng. J. 409 (2021) 128235, https://doi.org/10.1016/J.CEJ.2020.128235.
[61] S.Y. Shajaripour Jaberi, A. Ghaffarinejad, Z. Khajehsaeidi, A. Sadeghi, The synthesis, properties, and potential applications of CoS_2 as a transition metal dichalcogenide (TMD), Int. J. Hydrogen Energy 48 (2023) 15831–15878, https://doi.org/10.1016/J.IJHYDENE.2023.01.056.
[62] J. Zhu, L. Xiang, D. Xi, Y. Zhou, J. Yang, One-step hydrothermal synthesis of flower-like CoS hierarchitectures for application in supercapacitors, Bull. Mater. Sci. 41 (2018) 54, https://doi.org/10.1007/s12034-018-1570-x.
[63] C. Sambathkumar, N. Nallamuthu, M.K. Kumar, S. Sudhahar, P. Devendran, Electrochemical exploration of cobalt sulfide nanoparticles synthesis using cobalt diethyldithiocarbamate as single source precursor for hybrid supercapacitor device, J. Alloys Compd. 920 (2022) 165839, https://doi.org/10.1016/J.JALLCOM.2022.165839.
[64] R. Ren, M. Faber, R. Dziedzic, Z. Wen, S. Jin, S. Mao, J. Chen, Metallic CoS_2 nanowire electrodes for high cycling performance supercapacitors, Nanotechnology 26 (2015) 494001, https://doi.org/10.1088/0957-4484/26/49/494001.
[65] J. Li, K.S. Hui, Y. Zheng, S. Ji, K. Wang, C. Zha, D.A. Dinh, X. Fan, F. Chen, Z. Shao, K.N. Hui, Stabilizing anionic redox processes in electrospun NiS_2–based cathode towards durable aluminum-ion batteries, Chem. Eng. J. 450 (2022) 138237, https://doi.org/10.1016/J.CEJ.2022.138237.
[66] T. Wang, P. Hu, C. Zhang, H. Du, Z. Zhang, X. Wang, S. Chen, J. Xiong, G. Cui, Nickel disulfide–graphene nanosheets composites with improved electrochemical performance for sodium ion battery, ACS Applied Materials & Interfaces 8 (2016) 7811–7817, https://doi.org/10.1021/acsami.6b00179.
[67] L. Li, Y. Ma, F. Cui, Y. Li, D. Yu, X. Lian, Y. Hu, H. Li, S. Peng, Novel insight into rechargeable aluminum batteries with promising selenium sulfide@carbon nanofibers cathode, Adv. Mater. 35 (2022), https://doi.org/10.1002/adma.202209628.
[68] V.H. Pham, J.A. Boscoboinik, D.J. Stacchiola, E.C. Self, P. Manikandan, S. Nagarajan, Y. Wang, V.G. Pol, J. Nanda, E. Paek, D. Mitlin, Selenium-sulfur (SeS) fast charging cathode for sodium and lithium metal batteries, Energy Storage Mater. 20 (2019) 71–79, https://doi.org/10.1016/J.ENSM.2019.04.021.
[69] Z. Zhao-Karger, X.M. Lin, C. Bonatto Minella, D. Wang, T. Diemant, R.J. Behm, M. Fichtner, Selenium and selenium-sulfur cathode materials for high-energy rechargeable magnesium batteries, J. Power Sources 323 (2016) 213–219, https://doi.org/10.1016/J.JPOWSOUR.2016.05.034.
[70] G.-L. Xu, J. Liu, R. Amine, Z. Chen, K. Amine, Selenium and selenium–sulfur chemistry for rechargeable lithium batteries: interplay of cathode structures, electrolytes, and interfaces, ACS Energy Lett. 2 (2017) 605–614, https://doi.org/10.1021/acsenergylett.6b00642.
[71] Y. Zhang, S. Jiang, Y. Li, X. Ren, P. Zhang, L. Sun, H.Y. Yang, In situ grown hierarchical electrospun nanofiber skeletons with embedded vanadium nitride nanograins for ultra-fast and super-long cycle life aqueous Zn-ion batteries, Adv. Energy Mater. 13 (2023) 2202826, https://doi.org/10.1002/aenm.202202826.
[72] H. Chen, Z. Yang, J. Wu, Vanadium nitride@nitrogen-doped graphene as zinc ion battery cathode with high rate capability and long cycle stability, Industrial & Engineering Chemistry Research 61 (2022) 2955–2962, https://doi.org/10.1021/acs.iecr.1c04683.
[73] Y. Rong, H. Chen, J. Wu, Z. Yang, L. Deng, Z. Fu, Granular vanadium nitride (VN) cathode for high-capacity and stable zinc-ion batteries, Industrial & Engineering Chemistry Research 60 (2021) 8649–8658, https://doi.org/10.1021/acs.iecr.1c01052.
[74] M. Pandurangan, R. Ponraj, J.H. Yun, D.-K. Kim, Electrochemical performance of vanadium nitride/carbon/N-doped MWCNT as anode materials for lithium-ion batteries, in: ECS Meeting Abstracts. MA2020-02, 2020, p. 244, https://doi.org/10.1149/MA2020-022244mtgabs.
[75] A. Morel, Y. Borjon-Piron, R.L. Porto, T. Brousse, D. Bélanger, Suitable conditions for the use of vanadium nitride as an electrode for electrochemical capacitor, J. Electrochem. Soc. 163 (2016) A1077–A1082, https://doi.org/10.1149/2.1221606jes.
[76] Y.C. Wu, W.R. Liu, Few-layered $MoSe_2$ ultrathin nanosheets as anode materials for lithium ion batteries, J. Alloys Compd. 813 (2020) 152074, https://doi.org/10.1016/J.JALLCOM.2019.152074.
[77] X. Ji, M. Li, J. Guo, Y. Pan, L. Meng, S. Cheng, Development and enhancement strategy of $MoSe_2$ based anodes for aqueous Li-ion battery, Journal of Science: Advanced Materials and Devices 7 (2022) 100455, https://doi.org/10.1016/J.JSAMD.2022.100455.
[78] L. Tang, B. Zhang, C. An, H. Li, B. Xiao, J. Li, Z. He, J. Zheng, Ultrahigh-rate behavior anode materials of $MoSe_2$ nanosheets anchored on dual-heteroatoms functionalized graphene for sodium-ion batteries, Inorg. Chem. 58 (2019) 8169–8178, https://doi.org/10.1021/acs.inorgchem.9b00971.
[79] P. Ge, L. Zhang, Y. Yang, W. Sun, Y. Hu, X. Ji, Advanced $MoSe_2$/carbon electrodes in Li/Na-ions batteries, Adv. Mater. Interfaces 7 (2020) 1901651, https://doi.org/10.1002/admi.201901651.
[80] H. Yang, H. Li, J. Li, Z. Sun, K. He, H.M. Cheng, F. Li, The rechargeable aluminum battery: opportunities and challenges, Angewandte Chemie - International Edition 58 (2019) 11978–11996, https://doi.org/10.1002/anie.201814031.
[81] W. Yang, H. Lu, Y. Cao, P. Jing, X. Hu, H. Yu, A flexible free-standing cathode based on graphene-like $MoSe_2$ nanosheets anchored on N-doped carbon nanofibers for rechargeable aluminum-ion batteries, Ionics (Kiel) 26 (2020), https://doi.org/10.1007/s11581-020-03476-x.
[82] X. Li, W. Lv, G. Wu, G. Fu, W. Zhang, Z. Li, A novel CuSe-Cu1.8Se heterostructure with hexahedral structure cathode material for aluminum batteries, Chem. Eng. J. 426 (2021) 131899, https://doi.org/10.1016/J.CEJ.2021.131899.
[83] X. Huo, J. Liu, J. Li, B. Zhang, Y. Zhang, Y. Yu, F. Kang, Hexagonal composite CuSe@C as a positive electrode for high-performance aluminum batteries, ACS Appl Energy Mater. 3 (2020) 11445–11455, https://doi.org/10.1021/acsaem.0c02374.
[84] M. Hayat, Y. Zhou, M.Z. Ullah Shah, M. Sana Ullah, M.B. Hanif, H. Hou, U. Arif, S. Khan, A.M. Hassan, A.M. Tighezza, M. Sajjad, R. Vadla, Exploring the electrochemical properties of CuSe-decorated NiSe2 nanocubes for battery-supercapacitor hybrid devices, Chemosphere 340 (2023) 139720, https://doi.org/10.1016/J.CHEMOSPHERE.2023.139720.
[85] G. Li, M. Kou, J. Tu, Y. Luo, M. Wang, S. Jiao, Coordination interaction boosts energy storage in rechargeable Al battery with a positive electrode material of CuSe, Chem. Eng. J. 421 (2021) 127792, https://doi.org/10.1016/J.CEJ.2020.127792.
[86] Z. Zhou, W. Zhang, W. Zhao, Z. Yang, C. Zeng, A replacement etching route to CuSe with a hierarchical hollow structure for enhanced performance in lithium ion batteries, J. Electron. Mater. 43 (2014) 359–368, https://doi.org/10.1007/s11664-013-2905-4.

[87] C. Chen, Q. Hu, F. Yang, H. Xue, Y. Zhang, H. Yan, Y. Lu, Y. Luo, A facile synthesis of CuSe nanosheets for high-performance sodium-ion hybrid capacitors, RSC Adv. 12 (2022) 21558–21566, https://doi.org/10.1039/D2RA03206F.
[88] C. Zhang, X. Yang, L. Chai, W. Zhang, Z. Li, Novel $Cu_{1.8}Se$ carbon fiber composite for aluminum-ion battery cathode materials: outstanding electrochemical performance, Compos B Eng. 249 (2023) 110411, https://doi.org/10.1016/J.COMPOSITESB.2022.110411.
[89] J. Long, Z. Yang, F. Yang, J. Cuan, J. Wu, Electrospun core-shell Mn_3O_4/carbon fibers as high-performance cathode materials for aqueous zinc-ion batteries, Electrochim. Acta 344 (2020) 136155, https://doi.org/10.1016/J.ELECTACTA.2020.136155.
[90] F. Tang, T. He, H. Zhang, X. Wu, Y. Li, F. Long, Y. Xiang, L. Zhu, J. Wu, X. Wu, The MnO@N-doped carbon composite derived from electrospinning as cathode material for aqueous zinc ion battery, J. Electroanal. Chem. 873 (2020) 114368, https://doi.org/10.1016/J.JELECHEM.2020.114368.
[91] L. Ding, J. Gao, T. Yan, C. Cheng, L.-Y. Chang, N. Zhang, X. Feng, L. Zhang, Boosting the cycling stability of aqueous zinc-ion batteries through nanofibrous coating of a bead-like MnO_x cathode, ACS Applied Materials & Interfaces 14 (2022) 17570–17577, https://doi.org/10.1021/acsami.2c03170.
[92] L. Cheng, Y. Wu, S. Guo, Y. Liu, W. Li, Q. Liu, F. Mo, S. Yu, Y. Huang, J. Wei, Electrospun manganese sesquioxide as cathode for aqueous zinc ion battery with high-rate performance and long cycle life, Mater. Lett. 327 (2022) 132920, https://doi.org/10.1016/J.MATLET.2022.132920.
[93] A.U. Ubale, M.A. Waghmare, K.S. Iqbal, H.M. Pathan, Manganese oxides: promising electrode materials for Li-ion batteries and supercapacitors, J. Mater. Sci. Mater. Electron. 31 (2020) 14003–14021, https://doi.org/10.1007/s10854-020-04033-y.
[94] T.M. Narayanan, Y.G. Zhu, E. Gençer, G. McKinley, Y. Shao-Horn, Low-cost manganese dioxide semi-solid electrode for flow batteries, Joule 5 (2021) 2934–2954, https://doi.org/10.1016/J.JOULE.2021.07.010.
[95] D. Bélanger, T. Brousse, J. Long, Manganese oxides: battery materials make the leap to electrochemical capacitors, Electrochem. Soc. Interface 17 (2008) 49–52, https://doi.org/10.1149/2.F07081IF.
[96] H. Chen, W. Zhou, D. Zhu, Z. Liu, Z. Feng, J. Li, Y. Chen, Porous cube-like Mn_3O_4@C as an advanced cathode for low-cost neutral zinc-ion battery, J. Alloys Compd. 813 (2020) 151812, https://doi.org/10.1016/J.JALLCOM.2019.151812.
[97] C. Yin, J. Chen, C.-L. Pan, Y. Pan, J. Hu, MOF-derived Mn_3O_4@C hierarchical nanospheres as cathodes for aqueous zinc-ion batteries, ACS Appl Energy Mater. 5 (2022) 14144–14154, https://doi.org/10.1021/acsaem.2c02690.
[98] L. Wang, L. Li, H. Wang, J. Yang, F. Wu, R. Chen, Stable conversion Mn_3O_4 Li-ion battery anode material with integrated hierarchical and core–shell structure, ACS Appl Energy Mater. 2 (2019) 5206–5213, https://doi.org/10.1021/acsaem.9b00839.
[99] N. Harudin, Z. Osman, S.R. Majid, R. Rosli, Electrospun of $MgMn_2O_4$ based cathode materials for rechargeable magnesium ion cells, Mol. Cryst. Liq. Cryst. 759 (2023) 44–52, https://doi.org/10.1080/15421406.2022.2160903.
[100] X. Zhang, X. Sun, X. Li, X. Hu, S. Cai, C. Zheng, Recent progress in rate and cycling performance modifications of vanadium oxides cathode for lithium-ion batteries, Journal of Energy Chemistry 59 (2021) 343–363, https://doi.org/10.1016/J.JECHEM.2020.11.022.
[101] Y. Kim, Y. Park, M. Kim, J. Lee, K.J. Kim, J.W. Choi, Corrosion as the origin of limited lifetime of vanadium oxide-based aqueous zinc ion batteries, Nat. Commun. 13 (2022) 2371, https://doi.org/10.1038/s41467-022-29987-x.
[102] F. Mattelaer, K. Geryl, G. Rampelberg, J. Dendooven, C. Detavernier, Amorphous and crystalline vanadium oxides as high-energy and high-power cathodes for three-dimensional thin-film Lithium ion batteries, ACS Applied Materials & Interfaces 9 (2017) 13121–13131, https://doi.org/10.1021/acsami.6b16473.
[103] X. Chen, Q. Kong, X. Wu, X. An, J. Zhang, Q. Wang, W. Yao, V_2O_3@C optimized by carbon regulation strategy for ultra long-life aqueous zinc-ion batteries, Chem. Eng. J. 451 (2023) 138765, https://doi.org/10.1016/J.CEJ.2022.138765.
[104] T. Zhou, Q. Han, L. Xie, X. Yang, L. Zhu, X. Cao, Recent developments and challenges of vanadium oxides (V_xO_y) cathodes for aqueous zinc-ion batteries, Chem. Rec. 22 (2022) e202100275, https://doi.org/10.1002/tcr.202100275.
[105] X. Zhang, F. Xue, X. Sun, T. Hou, Z. Xu, Y. Na, Q. An, Z. Chen, S. Cai, C. Zheng, High-capacity zinc vanadium oxides with long-term cyclability enabled by in-situ electrochemical oxidation as zinc-ion battery cathode, Chem. Eng. J. 445 (2022) 136714, https://doi.org/10.1016/J.CEJ.2022.136714.
[106] L. Deng, H. Chen, J. Wu, Z. Yang, Y. Rong, Z. Fu, V_2O_3 as cathode of zinc ion battery with high stability and long cycling life, Ionics (Kiel) 27 (2021), https://doi.org/10.1007/s11581-021-04121-x.
[107] T. Han, Y. Wang, H. Bai, H. Zhang, J. Liu, A lamellar V_2O_3@C composite for aluminium-ion batteries displaying long cycle life and low-temperature tolerance, Chem. Commun. 58 (2022) 7172–7175, https://doi.org/10.1039/D2CC01931K.
[108] X. Liu, G. Li, J. Wu, D. Zhang, L. Li, Fabrication of VO nanorings on a porous carbon architecture for high-performance Li-ion batteries, ACS Applied Materials & Interfaces 14 (2022) 9454–9463, https://doi.org/10.1021/acsami.1c22915.
[109] H. Wang, S. Zhang, C. Deng, In situ encapsulating metal oxides into core–shell hierarchical hybrid fibers for flexible zinc-ion batteries toward high durability and ultrafast capability for wearable applications, ACS Applied Materials & Interfaces 11 (2019) 35796–35808, https://doi.org/10.1021/acsami.9b13537.
[110] X. Chen, L. Wang, H. Li, F. Cheng, J. Chen, Porous V_2O_5 nanofibers as cathode materials for rechargeable aqueous zinc-ion batteries, Journal of Energy Chemistry 38 (2019) 20–25, https://doi.org/10.1016/J.JECHEM.2018.12.023.
[111] Z. Chen, J. Hu, S. Liu, H. Hou, G. Zou, W. Deng, X. Ji, Dual defects boosting zinc ion storage of hierarchical vanadium oxide fibers, Chem. Eng. J. 404 (2021) 126536, https://doi.org/10.1016/J.CEJ.2020.126536.
[112] G. Yoo, B.R. Koo, H.R. An, C. Huang, G.H. An, Enhanced and stabilized charge transport boosting by Fe-doping effect of V_2O_5 nanorod for rechargeable Zn-ion battery, J. Ind. Eng. Chem. 99 (2021) 344–351, https://doi.org/10.1016/J.JIEC.2021.04.041.
[113] G. Yoo, G.H. Ryu, B.R. Koo, G.H. An, Interfacial defect engineering via combusted graphene in V_2O_5 nanochips to develop high-rate and stable zinc-ion batteries, Ceram. Int. 47 (2021) 31817–31825, https://doi.org/10.1016/J.CERAMINT.2021.08.064.
[114] N. Xu, C. Yan, W. He, L. Xu, Z. Jiang, A. Zheng, H. Wu, M. Chen, G. Diao, Flexible electrode material of V_2O_5 carbon fiber cloth for enhanced zinc ion storage performance in flexible zinc-ion battery, J. Power Sources 533 (2022) 231358, https://doi.org/10.1016/J.JPOWSOUR.2022.231358.
[115] A.I. Volkov, A.S. Sharlaev, O.Ya. Berezina, E.G. Tolstopjatova, L. Fu, V. V. Kondratiev, Electrospun V_2O_5 nanofibers as high-capacity cathode materials for zinc-ion batteries, Mater. Lett. 308 (2022) 131212, https://doi.org/10.1016/J.MATLET.2021.131212.
[116] X. Liu, Z. Wang, Y. Niu, C. Liu, H. Chen, X. Ren, Z. Liu, W.-M. Lau, D. Zhou, Electrospun V_2O_3@carbon nanofibers as a flexible and binder-free cathode for highly stable aqueous Zn-ion full batteries, ACS Appl Energy Mater. 5 (2022) 3525–3535, https://doi.org/10.1021/acsaem.1c04068.
[117] J. Liu, L. Zhan, K. Sun, K. Huang, T. Wei, C. Wang, Electrospinning preparation of a high-rate self-supported cathode for rechargeable aqueous zinc-ion batteries, Energy Fuel 36 (2022), https://doi.org/10.1021/acs.energyfuels.2c02633.
[118] D. Liepinya, R. Shepard, M. Smeu, 2D $Ni_{0.25}Mn_{0.75}O_2$: a high-performance cathode for multivalent ion batteries, Comput. Mater. Sci. 202 (2022) 110948, https://doi.org/10.1016/J.COMMATSCI.2021.110948.
[120] Z. Zhang, X. Zhang, X. Zhao, S. Yao, A. Chen, Z. Zhou, Computational screening of layered materials for multivalent ion batteries, ACS Omega 4 (2019) 7822–7828, https://doi.org/10.1021/acsomega.9b00482.
[121] Z. Liu, Y. Gu, L. Bi, Applications of electrospun nanofibers in solid oxide fuel cells – a review, J. Alloys Compd. 937 (2023) 168288, https://doi.org/10.1016/J.JALLCOM.2022.168288.
[122] S. Kalluri, K.H. Seng, Z. Guo, H.K. Liu, S.X. Dou, Electrospun lithium metal oxide cathode materials for lithium-ion batteries, RSC Adv. 3 (2013) 25576–25601, https://doi.org/10.1039/C3RA45414B.
[123] S.N. Banitaba, A. Ehrmann, Application of electrospun nanofibers for fabrication of versatile and highly efficient electrochemical devices: a review, Polymers (Basel) 13 (2021), https://doi.org/10.3390/polym13111741.
[124] M. Baghali, W.A.D.M. Jayathilaka, S. Ramakrishna, The role of electrospun nanomaterials in the future of energy and environment, Materials 14 (2021) 1–53, https://doi.org/10.3390/ma14030558.
[125] B. Joshi, E. Samuel, Y. Kim, A.L. Yarin, M.T. Swihart, S.S. Yoon, Progress and potential of electrospinning-derived substrate-free and binder-free lithium-ion battery electrodes, Chem. Eng. J. 430 (2022) 132876, https://doi.org/10.1016/j.cej.2021.132876.
[126] K. Shen, S. Zhai, S. Wang, Q. Ru, X. Hou, K. San Hui, K. Nam Hui, F. Chen, Recent progress in binder-free electrodes synthesis for electrochemical energy storage application, Batter Supercaps 4 (2021) 860–880, https://doi.org/10.1002/batt.202000271.
[127] Y. Zhao, J. Yan, J. Yu, B. Ding, Electrospun nanofiber electrodes for lithium-ion batteries, Macromol. Rapid Commun. 44 (2023) 2200740, https://doi.org/10.1002/marc.202200740.
[128] A. Singh, V. Kalra, Electrospun nanostructures for conversion type cathode (S, Se) based lithium and sodium batteries, J Mater Chem A Mater. 7 (2019) 11613–11650, https://doi.org/10.1039/C9TA00327D.
[129] P. Sun, X. Zhao, R. Chen, T. Chen, L. Ma, Q. Fan, H. Lu, Y. Hu, Z. Tie, Z. Jin, Q. Xu, J. Liu, $Li_3V_2(PO_4)_3$ encapsulated flexible free-standing nanofabric cathodes for fast charging and long life-cycle lithium-ion batteries, Nanoscale 8 (2016) 7408–7415, https://doi.org/10.1039/C5NR08832A.
[130] B. Sahoo, P.K. Panda, S. Ramakrishna, Electrospinning of functional ceramic nanofibers, Open Ceramics 11 (2022) 100291, https://doi.org/10.1016/J.OCERAM.2022.100291.
[131] A. La Monaca, A. Paolella, A. Guerfi, F. Rosei, K. Zaghib, Electrospun ceramic nanofibers as 1D solid electrolytes for lithium batteries, Electrochem. Commun. 104 (2019) 106483, https://doi.org/10.1016/J.ELECOM.2019.106483.
[132] P. Pintauro, R. Wycisk, A.N. Mondal, J. Waugh, G. Liu, J. Nanda, High-Performance Li-Ion Battery Anodes From Electrospun Nanoparticle/Conducting Polymer Nanofibers, United States, 2021, https://doi.org/10.2172/1603318.
[133] X. Zhang, L. Ji, O. Toprakci, Y. Liang, M. Alcoutlabi, Electrospun nanofiber-based anodes, cathodes, and separators for advanced lithium-ion batteries, Polym. Rev. 51 (2011) 239–264, https://doi.org/10.1080/15583724.2011.593390.
[134] V. Charkhesht, B. Yarar Kaplan, S. Alkan Gürsel, A. Yürüm, Electrospun nanotubular titania and polymeric interfaces for high energy density Li-ion electrodes, Energy & Fuels 37 (2023) 6197–6207, https://doi.org/10.1021/acs.energyfuels.3c00192.
[135] J. Wang, Z. Wang, J. Ni, L. Li, Electrospun materials for batteries moving beyond lithium-ion technologies, Electrochemical Energy Reviews 5 (2022) 211–241, https://doi.org/10.1007/s41918-021-00103-9.
[136] W. Lei, H. Li, Y. Tang, H. Shao, Progress and perspectives on electrospinning techniques for solid-state lithium batteries, Carbon Energy 4 (2022) 539–575, https://doi.org/10.1002/cey2.180.
[138] C. Xia, Y. Zhou, C. He, A.I. Douka, W. Guo, K. Qi, B.Y. Xia, Recent advances on electrospun nanomaterials for zinc–air batteries, Small Science 1 (2021) 2100010, https://doi.org/10.1002/smsc.202100010.

[139] Y. Yan, X. Liu, J. Yan, C. Guan, J. Wang, Electrospun nanofibers for new generation flexible energy storage, Energy & Environmental Materials 4 (2021) 502–521, https://doi.org/10.1002/eem2.12146.
[140] F. Shi, C. Chen, Z.-L. Xu, Recent advances on electrospun nanofiber materials for post-lithium ion batteries, Advanced Fiber Materials 3 (2021) 275–301, https://doi.org/10.1007/s42765-021-00070-2.
[141] B. Zhang, F. Kang, J.-M. Tarascon, J.-K. Kim, Recent advances in electrospun carbon nanofibers and their application in electrochemical energy storage, Prog. Mater. Sci. 76 (2016) 319–380, https://doi.org/10.1016/j.pmatsci.2015.08.002.
[142] G. Nie, X. Zhao, Y. Luan, J. Jiangmin, K. Kui, J. Wang, Key issues facing electrospun carbon nanofibers in energy applications: on-going approaches and challenges, Nanoscale 12 (2020), https://doi.org/10.1039/D0NR03425H.
[143] S. Cavaliere, S. Subianto, I. Savych, D.J. Jones, J. Rozière, Electrospinning: designed architectures for energy conversion and storage devices, Energy Environ. Sci. 4 (2011) 4761–4785, https://doi.org/10.1039/C1EE02201F.
[144] T. Koketsu, J. Ma, B.J. Morgan, M. Body, C. Legein, W. Dachraoui, M. Giannini, A. Demortière, M. Salanne, F. Dardoize, H. Groult, O.J. Borkiewicz, K. W. Chapman, P. Strasser, D. Dambournet, Reversible magnesium and aluminium ions insertion in cation-deficient anatase TiO_2, Nat. Mater. 16 (2017) 1142–1148, https://doi.org/10.1038/nmat4976.
[145] Y. Tong, X. Li, S. Su, J. Li, J. Fang, B. Liang, J. Hou, M. Luo, Hydrated lithium ions intercalated V_2O_5 with dual-ion synergistic insertion mechanism for high-performance aqueous zinc-ion batteries, J. Colloid Interface Sci. 606 (2022) 645–653, https://doi.org/10.1016/j.jcis.2021.08.051.
[146] R. Cang, C. Zhao, K. Ye, J. Yin, K. Zhu, J. Yan, G. Wang, D. Cao, Aqueous calcium-ion battery based on a mesoporous organic anode and a manganite cathode with long cycling performance, ChemSusChem 13 (2020) 3911–3918, https://doi.org/10.1002/cssc.202000812.
[147] R.J. Gummow, G. Vamvounis, M.B. Kannan, Y. He, Calcium-ion batteries: current state-of-the-art and future perspectives, Adv. Mater. 30 (2018) 1801702, https://doi.org/10.1002/adma.201801702.
[148] S. Gheytani, Y. Liang, F. Wu, Y. Jing, H. Dong, K.K. Rao, X. Chi, F. Fang, Y. Yao, An aqueous ca-ion battery, Adv. Sci. 4 (2017) 1700465, https://doi.org/10.1002/advs.201700465.
[149] Md. Adil, A. Sarkar, A. Roy, M. Ranjan Panda, A. Nagendra, S. Mitra, Practical aqueous calcium-ion battery full-cells for future stationary storage, ACS Applied Materials & Interfaces 12 (2020) 11489–11503, https://doi.org/10.1021/acsami.9b20129.
[150] Z.-L. Xu, J. Park, J. Wang, H. Moon, G. Yoon, J. Lim, Y.-J. Ko, S.-P. Cho, S.-Y. Lee, K. Kang, A new high-voltage calcium intercalation host for ultra-stable and high-power calcium rechargeable batteries, Nat. Commun. 12 (2021) 3369, https://doi.org/10.1038/s41467-021-23703-x.